# EFFECTS OF VEGETATION STRUCTURE AND CANOPY EXPOSURE ON SMALL-SCALE VARIATION IN ATMOSPHERIC DEPOSITION INPUTS TO A MIXED CONIFER FOREST IN CALIFORNIA

Kereen Griffith

Thesis Prepared for the Degree of

MASTER OF SCIENCE

UNIVERSITY OF NORTH TEXAS

May 2014

APPROVED:

Alexandra Ponette-González, Major Professor
Pinliang Dong, Committee Member
Barney Venables, Committee Member
Paul Hudak, Chair of the Department of Geography
Mark Wardell, Dean of the Toulouse Graduate School

Griffith, Kereen. Effects of Vegetation Structure and Canopy Exposure on Small-Scale Variation in Atmospheric Deposition Inputs to a Mixed Conifer Forest in California. Master of Science (Applied Geography), May 2014, 67 pp., 8 tables, 10 figures, references, 113 titles.

Data on rates of atmospheric deposition is limited in many montane ecosystems, where high spatial variability in meteorological, topographic, and vegetation factors contributes to elevated atmospheric inputs and to the creation of deposition hotspots. Addressing the ecological consequences of increasing deposition in these areas will require a better understanding of surface controls influencing atmospheric deposition rates at both large and small-scales.

The overarching objective of this thesis research was to understand the influence of vegetation structure and canopy exposure on small-scale patterns of atmospheric sulfate, nitrate, and chloride deposition inputs to a conifer forest in the Santa Cruz Mountains, California. Throughfall ion fluxes (i.e., ions delivered in water that pass from the forest canopy to the forest floor), bulk deposition (i.e., primarily wet deposition), and rainfall data were collected during the rainy period from October 2012 to May 2013. Throughfall $SO_4^{2-}$, $Cl^-$, and $NO_3^-$ fluxes were measured beneath eight clusters of Douglas fir (*Pseudotsuga menziesii*) trees (three trees per cluster) differing in tree size (i.e., diameter at breast height; DBH) and canopy exposure. In each cluster, a throughfall collector was placed 1-meter from the bole of an individual tree, for a total of 24 individual collectors. The position of each throughfall collector was recorded with a Trimble® GPS. In addition, tree height, tree diameter, and leaf area index, were measured for all trees. LiDAR data were obtained from GeoEarthScope's Northern California Airborne LiDAR project and used to model the elevation (DEM), canopy surface

height (DSM), tree height (CHM), slope, and curvature of the canopy surface across the entire study area.

Over the rainy season, total throughfall flux of $SO_4^{2-}$-S, a conservative tracer of total deposition (wet + dry + fog), to Douglas fir clusters ranged from 1.44 - 3.84 kg S $ha^{-1}$ wet $season^{-1}$, while dry and fog deposition ranged from 0.13 -2.37 kg S $ha^{-1}$ wet $season^{-1}$. Total deposition to exposed mature tree clusters was 1.7-2.7 times higher than other clusters. Patterns of total $Cl^-$ fluxes (17.10 – 54.14 kg $Cl^-$ $ha^{-1}$ wet $season^{-1}$) resembled patterns of total $SO_4^{2-}$-S inputs. Overall, net throughfall fluxes (throughfall – bulk deposition) to Douglas fir trees clusters were more variable than total throughfall fluxes. Net $SO_4^{2-}$-S and $Cl^-$ fluxes to individual collectors increased with tree DBH and the convexity of the canopy surface. Compared to $SO_4^{2-}$-S and $Cl^-$ in throughfall, total $NO_3^-$-N fluxes (0.17 - 4.03 kg N $ha^{-1}$ wet $season^{-1}$) were low and appeared to vary with small-scale changes in elevation. Geospatial technologies and remote sensing tools, such as LiDAR, are promising in the study of relationships between atmospheric deposition and topography (including vegetation), and in scaling-up estimates of atmospheric deposition to larger spatial scales. Understanding small-scale surface controls on atmospheric deposition has implications for different areas of research within geography, including modeling the spread of emerging infectious disease and assessing the effects of nitrogen cycling on native and invasive plant species composition.

ACKNOWLEDGMENTS

I would like to express sincere gratitude to my major advisor, Dr. Alexandra Ponette-González, for her generous support and professional guidance throughout the entirety of this research project. I would also like to extend thanks to Dr. Pinliang Dong for his assistance with LiDAR, Dr. Barney Venables for sampling recommendations, Bethel Steele for her tireless support in the field and laboratory, and the staff at the Cary Institute of Ecosystem Studies Analytical Laboratory for assistance with chemical analysis. I would also like to acknowledge Edgar Orre, Angela Bernheisel, and the California Department of Forestry and Protection (Cal Fire) staff for their assistance with field sampling. Finally, I would like to thank my family for their unwavering encouragement and support throughout my study. Funding for this research was provided by the NASA Land Cover/Land-Use Change Program (to L.M. Curran and A.G. Ponette-González NNX11AF08G).

TABLE OF CONTENTS

Page

LIST OF TABLES

Page

LIST OF FIGURES

Page

# CHAPTER 1

# ATMOSPHERIC DEPOSTION IN MONTANE FORESTS

## The Importance of Atmospheric Deposition

Atmospheric deposition (i.e., the movement of nutrients and pollutants from the atmosphere to the Earth's surface) is a vital component of nutrient cycling in forest ecosystems (Fenn et al. 2010, Fowler et al. 1984, Lovett 1994, Weathers et al. 1998, Weathers and Ponette-González 2011). Primary production in forest ecosystems is limited by the availability of essential macro- and micronutrients, some of which are deposited in significant quantities in rain and snow (i.e., wet deposition), as particles and gases (i.e., dry deposition), and in fog (i.e., fog deposition; Schlesinger et al. 2013). Total atmospheric deposition of any given nutrient or pollutant to an ecosystem is the sum of wet, dry, and fog deposition (Lovett 1994). In wet climates (e.g., tropical zones), total input is often dominated by wet deposition. However, in areas where rainfall is less frequent or where fog is prevalent, the relative contribution of dry and fog deposition to total deposition can be comparable to or greater than wet deposition (Weathers et al. 2006b).

The mechanisms of dry and fog deposition differ from wet deposition (Weathers et al. 1998). Large heavy rain droplets fall vertically to canopy surfaces due to gravity. Thus, wet deposition is primarily influenced by rainfall amount (Weathers and Ponette-González 2011). Large particles and gases not dissolved in water are deposited to canopy surfaces via sedimentation and impaction. Sedimentation occurs when particles suspended in the atmosphere settle on leaf, stem, and epiphyte surfaces. Whereas, impaction or interception of particles and gasses by leaf, stem, or epiphyte surfaces is more common at high wind speeds

(Erisman and Draaijers 2003, Lovett 1994). Small particles (i.e., less than about 0.2 micrometers) can directly penetrate leaf, stem, and epiphyte surfaces through molecular diffusion processes (i.e., movement of particles and gases from areas of high concentration to low concentration; Erisman and Draaijers 2003, Lovett 1994). Because of the different factors (e.g., meteorology, vegetation, and terrain features) controlling dry deposition of particles and gases in the atmosphere, dry deposition can vary considerably over small spatial scales (Lindberg and Lovett 1992, Lovett 1994). Compared to wet deposition, we know little about the controls on spatial patterns of dry and fog deposition at these small spatial scales. To investigate this question, my research focuses on the atmospheric deposition of sulfate-sulfur ($SO_4^{2-}$-S), chloride ($Cl^-$), and nitrate-nitrogen ($NO_3^-$-N) to Douglas fir (Pseudotsuga menziesii) tree canopies.

Sulfur, nitrogen, and chloride are essential nutrients for plant growth. Nitrogen is a primary macronutrient that often limits plant growth in temperate forest ecosystems (Vitousek 1982, Vitousek 1984). Sulfur and chloride are also essential for growth, but are used by plants in smaller quantities (Clarkson and Hanson 1980). Plants contain about 3% sulfur and 0.3% chloride relative to total nitrogen (George et al. 2008). In forest ecosystems, these nutrients are derived from natural as well as anthropogenic emission sources (Schlesinger et al. 2013). Major natural emission sources include; sea spray (e.g., $SO_4^{2-}$ and $Cl^-$), lightning (e.g., $NO_x$), and fire (e.g. release of sulfur, chloride, and nitrogen compounds). Biogenic processes, such as dimethyl sulfide production and plant and animal decomposition, are also important sources of sulfur and nitrogen (Seinfeld and Pandis 2012, Zhang et al. 2012). Major anthropogenic sources

include, fossil fuel combustion (e.g., $SO_2$, $Cl^-$, $NO_x$) and agricultural fertilization (e.g., $NH_3$; Chapin et al. 2012).

Increased anthropogenic activity has led to increases in atmospheric deposition of sulfur, chloride, and nitrogen throughout the world (Seinfeld and Pandis 2012). High levels of $SO_4^{2-}$, $Cl^-$, and $NO_3^-$ deposition in excess of plant requirements can inhibit plant growth and reduce biodiversity (Duarte et al. 2013, Fenn et al. 2010, Pajuste et al. 2006). In addition, studies have shown that elevated atmospheric deposition of these nutrients can cause soil acidification and nutrient enrichment (Bailey et al. 2005, Schaberg et al. 2002). Acidification (i.e., reduction in pH) of forest soils can alter soil microbial activity and cation exchange processes, leading to leaching of nutrients to nearby freshwater systems (Pardo et al. 2011). Nutrient enrichment can indirectly impact plant biodiversity in forest ecosystems by promoting the growth of nitrogen-tolerant invasive species over indigenous species (Fenn et al. 2005, Schaberg et al. 2002, Weathers et al. 1998). Therefore, atmospheric deposition of sulfur, chloride, and nitrogen to a forest ecosystem can contribute to increases in nutrient as well as pollutant loads.

## Atmospheric Deposition in Montane Environments

Mountains store and provide fresh water to nearly half of the world's population (Körner et al. 2005). Many of these areas are covered by forests, which store carbon and regulate surface runoff to freshwater streams (Körner 2004). Montane forests are biologically diverse ecosystems, encompassing different climate zones along elevational gradients. Nearly half of the world's biodiversity hotspots, biologically diverse areas threatened by anthropogenic activity, are also found in montane environments (Pickering et al. 2008).

Climatically, mountains are cooler, wetter, and windier compared to adjacent lowland areas (McNeill 2003). As a result, montane forests typically receive higher total deposition loads than neighboring lowland areas (Fowler et al. 1984, Igawa et al. 2001, Lovett 1994, Weathers et al. 2000; Table 1). High-elevation environments in the U.S., such as Yosemite National Park in California and the Great Smoky Mountains in Tennessee, continue to experience increases in atmospheric deposition that have the potential to decrease ecosystem productivity (Fenn et al. 2003, Johnson and Linberg 1992). Plant nutrient imbalances in montane forests resulting from soil acidification and nutrient enrichment can leave these ecosystems susceptible to multiple environmental stressors (i.e., pests and disease; Halman et al. 2008, Pugnaire and Luque 2001). Because of these potential impacts to montane forests, it is important to better understand spatial patterns of deposition, particularly in biologically diverse areas and areas susceptible to soil acidification and nutrient enrichment.

## Landscape-Scale Heterogeneity in Atmospheric Deposition

Although montane environments experience higher deposition rates than lowland areas, atmospheric deposition does not occur evenly across montane landscapes. At large spatial scales (i.e., greater than 1000 km), atmospheric deposition varies with proximity to emission source, topography, climate, and vegetation (Weathers and Ponette-González 2011; Table1). For example, montane forests near cities generally receive high $SO_4^{2-}$ and $NO_3^-$ loads from fossil fuel emissions, including emissions from industrial processes and vehicle exhaust, whereas montane forests near coastal areas receive high loads of $Cl^-$ and sodium ($Na^+$) from sea spray (Hedin et al. 1995, McDowell et al. 1990, Weathers et al. 1998). As mentioned above, high-elevation sites also receive higher amounts of wet and fog deposition as a result of

orographic precipitation and higher wind speeds at higher altitudes (Lindberg and Lovett 1992, Weathers et al. 2000). The relative amount of dry and fog deposition in montane landscapes vary with climate. In wet climates, wet deposition generally exceeds dry deposition fluxes, while in dry areas, or in areas seasonally immersed in fog, dry and fog deposition are comparable to or greater than wet deposition (Weathers et al. 2006b; Table 1). Finally, altitudinal zonation promotes distinct changes in tree species composition along elevational gradients (Stankwitz et al. 2012). Because needle leaves have greater leaf surface area than broadleaves, shifts in species composition at higher altitudes can increase dry and fog deposition inputs (Erisman and Draaijers 2003, Weathers et al., 2000; Table 1). Thus, there are many factors that contribute to spatial heterogeneity in atmospheric deposition in montane forest landscapes.

## Small-Scale Heterogeneity in Atmospheric Deposition

Atmospheric deposition also varies considerably over small spatial scales (i.e., less than 10s of kilometers), because meteorology, vegetation, and topography can change over very short horizontal and vertical distances (O'Brian et al. 2000, Weathers et al. 2001, Weathers et al. 2006a, Weathers et al. 2006b; Table 1). These factors can interact to create areas of increased deposition relative to the surrounding landscape (Ponette-Gonzalez et al. 2010). A better understanding of where these deposition "hotspots" are located or likely to occur is particularly important. This knowledge can improve critical load estimates. Critical loads are estimates of nutrient loads above which additional loads can be harmful to an ecosystem (Pardo et al. 2011). Atmospheric deposition of nutrients above an ecosystem's critical load limit can cause detrimental changes to water and soil chemistry (Fenn et al. 2005, Weathers et al.

1998). In addition, identifying vulnerable areas in a watershed or biologically diverse ecosystem can help in the management and protection of vital ecosystem services (Porter et al. 2005).

## Meteorological Patterns

Small-scale differences in meteorology (e.g., wind speed and wind direction) in montane landscapes are driven by changes in elevation, slope, and aspect within valleys and along ridges (i.e., slope crests; Mikita and Klimánek 2010). Local wind systems develop from diurnal temperature inversions: warm air flows upslope and up-valley during the day and cool air flows in the reverse direction at night (Lundquist and Cayan 2007; Fig. 1). These diurnal temperature inversions are similar to regional climate inversions that develop between high- and low-elevation environments (Daly et al. 2008). However, these changes are more difficult to measure, because of multiple factors associated with changes in wind speed and direction over short distances (Mikita and Klimánek 2010).

Topographic exposure and micro-relief characteristics also affect the velocity of different wind systems (Balestrini and Tagliaferri 2001). Topographic exposure is the exposure of a surface to prevailing winds relative to the surrounding area. Micro-relief characteristics include canopy surface roughness and the height of depressions and rises along slopes and in valleys. Slope, valley, and cross valley wind systems affect the dispersal of nutrients and pollutants present in air masses and contribute to the development of hotspots in areas that experience persistent turbulent air flow (Zimmermann et al. 2003; Fig. 1).

### *Topographic Position*

The topographic position of a site along a hillslope influences dry and fog deposition (Kirchner et al. 2014). For example, upslope positions along ridges are more exposed to the

atmosphere than downslope positions. Physical barriers blocking prevailing winds reduce deposition rates to downslope locations (Makowski Giannoni et al. 2013).

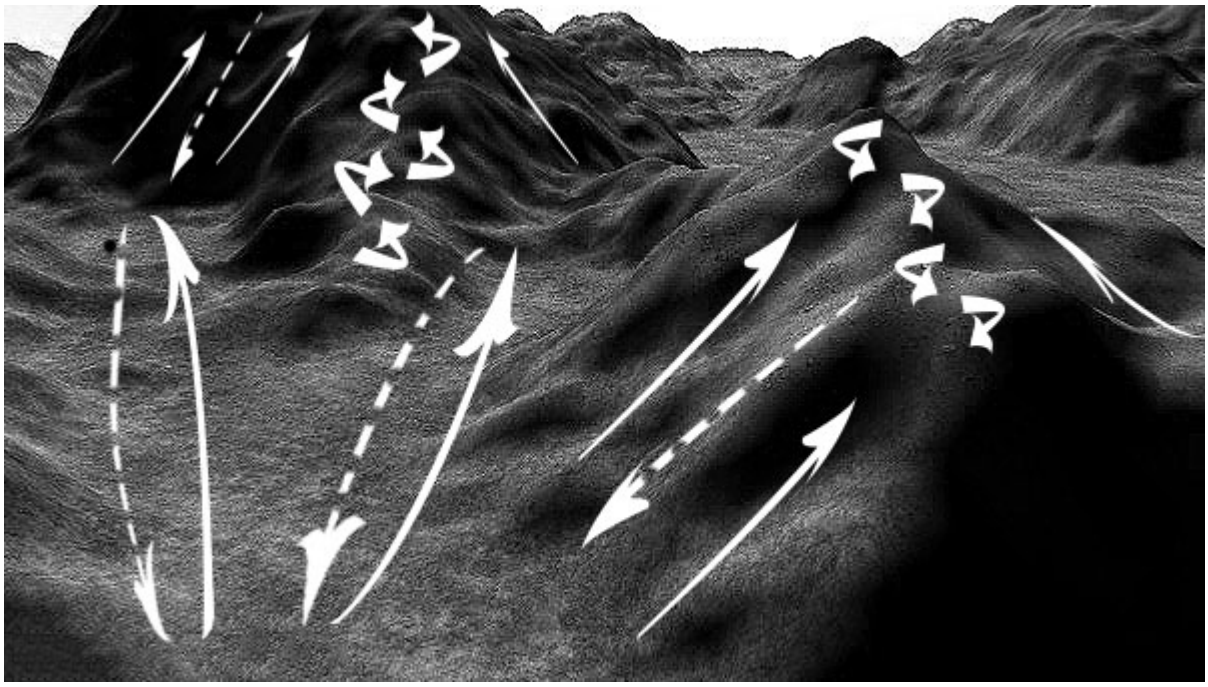

FIG. 1. Diagram of diurnal wind flow systems in a montane valley. Solid straight arrows indicate valley wind flow direction up-valley and upslope during the day. Dashed straight arrows indicate valley wind flow direction down-valley and downslope at night. Bent solid arrows indicate persistent turbulent wind flow where wind systems meet.

In contrast, exposed locations receive higher rates of deposition because of reduced sheltering from adjacent slopes (Chapman 2000). Turbulent airflow (i.e., irregular air flow that can easily diffuse through canopy openings) is also prevalent along slope ridges, because of interacting slope, valley, and cross-valley wind systems (Bitter et al. 1981; Fig. 1). Canopy interception of dry materials and fog droplets increases with turbulent airflow. Unlike laminar airflow (i.e., parallel straight air flow) characterized by reduced mixing, turbulent airflow can penetrate further into forest canopies, increasing exposed leaf surface area and increasing canopy interception (Katul et al. 2013).

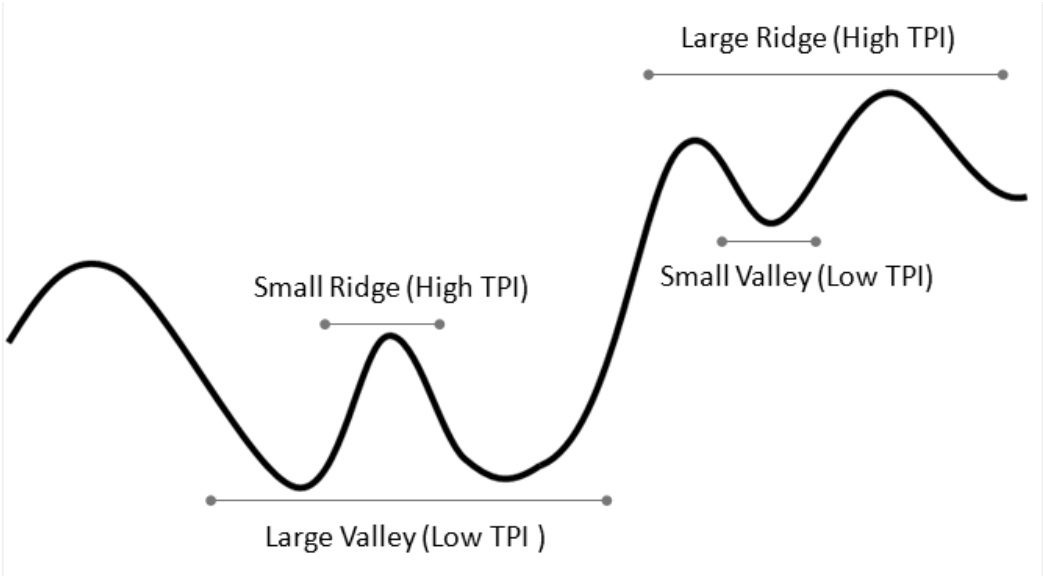


Fig. 2. Depiction of Topographic Position Index (TPI) in a montane landscape. Small ridges can experience high TPI relative to surrounding areas because of reduced sheltering from adjacent slopes. Similarly, small valleys at higher elevations can still experience low TPI relative to surroundings because of increased sheltering by adjacent slopes.

*Edge Effects*

Natural (e.g., fires, landslides, winds) and anthropogenic (e.g., road construction, logging) disturbances can create openings in forest canopies (Lindberg and Owen 1992). At the boundary between a forest and neighboring habitat, there are typically observable changes in microclimate, animal, and plant community structure (Cadenasso et al. 2003), which are referred to as "edge effects". In terms of vegetation structure, the creation of edges increases plant surface exposure to the atmosphere (Lindberg and Owen 1992) and also increases surface roughness and turbulent airflow (Bohrer et al. 2009), resulting in elevated deposition inputs at forest edges (Bohrer et al. 2009, Weathers et al. 2001; Table 1).

Weathers et al. (2000) also noted that "functional" edges can occur along steep slopes and in areas with large surface outcrops (Weathers et al. 2000; Fig. 3). They found increased

rates of dry and fog deposition along steep slopes (>20 degrees), similar to increased rates of dry and fog deposition observed near canopy gaps. Functional edges between ridges and along montane valley slopes may contribute to higher rates of dry and fog deposition at specific slope positions (Su et al. 2008).

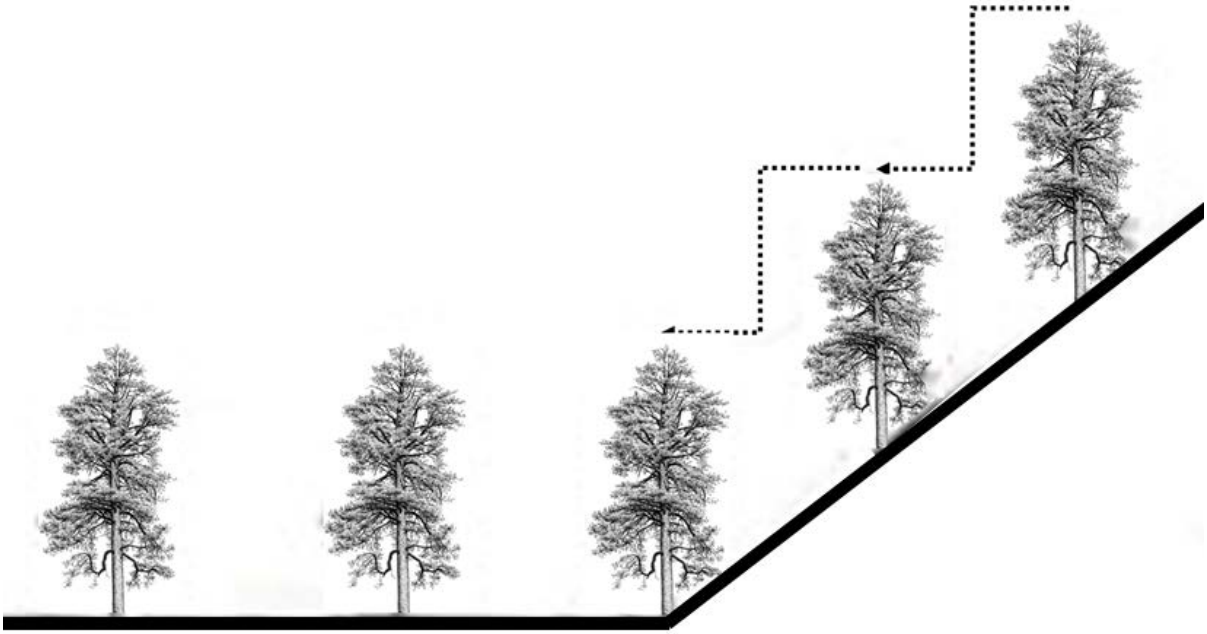

Fig. 3. Depiction of canopy roughness. Atmospheric deposition is greater along steep slopes than flat slopes, because of the influence of both horizontal and vertical displacement (dashed lines) between individual tree canopies.

*Canopy Roughness*

Atmospheric deposition increases as canopy roughness increases. Increased canopy roughness promotes turbulent mixing of air, which increases interception of gases, particles, and fog droplets by the forest canopy (Levia and Frost 2006, Maurer et al. 2013; Table 1). For example, in mixed evergreen forests, differences in tree height and vegetation density contribute to canopy roughness. Conifers have vertically elongated crowns that increase vertical displacement between adjacent broadleaf canopies (Erisman and Draaijers 2003).

Because changes in relief affect overall surface roughness, topography also affects the degree to which tree canopies are exposed to the atmosphere. In flat areas, trees located within small surface depressions are more protected from prevailing winds than trees on small rises that emerge above their neighbors. In montane forest environments, increased canopy roughness from changes in topography and canopy structure (e.g., tree height, LAI, and canopy closure) may interact to create deposition hotspots (Almquist et al. 2002, Hesp et al. 2013, Ponette-González et al. 2010, Weathers et al. 2006b).

## Measuring Atmospheric Deposition in Montane Forest Ecosystems

Due to the spatial heterogeneity of montane environments, there are logistical challenges involved in measuring atmospheric deposition inputs. Methods for measuring wet deposition include wet and bulk collection (Lovett 1994). Wet deposition collectors are automated systems that only open during periods of rainfall. In the United States, the National Atmospheric Deposition Program (NADP) uses wet deposition collectors to monitor wet deposition at over 300 sites across the conterminous United States (Nanus et al. 2012). These collection systems require electricity and are not easily established in remote montane environments (Fenn et al. 2009). Moreover, wet-only collectors underestimate wet deposition at high-elevation sites due to frequent snowfall and high wind speeds, which cause rain to be driven horizontally rather than vertically into collectors (Burns et al. 2003). Bulk collectors are open collection systems that primarily collect wet deposition and very small amounts of dry deposition that settle to collector surfaces. Because bulk collectors do not require electricity, they are often used in remote montane areas (Fenn et al. 2009). Water collected in bulk and wet deposition collectors are analyzed to determine ion concentrations in rainfall and then

multiplied by volume (i.e., precipitation) to calculate deposition over a given collector surface area (Weathers and Ponette-González 2011).

While wet deposition is easily measured with wet and bulk deposition collectors, other methods are required for measuring dry deposition (Fenn et al. 2009). Current methods for measuring dry deposition include the use of surrogate surfaces and inferential calculations. Though surrogate surfaces are useful for estimating dry and fog deposition to inert surfaces, surrogate surfaces do not accurately represent plant surface interactions (Caldwell et al. 2006, Lyman et al. 2007, Lyman et al. 2009). For the inferential method, dry deposition is calculated by multiplying air concentrations by deposition velocity. This method requires extensive data on air concentrations and meteorological conditions, but these data are often unavailable at montane sites (Adon et al. 2013, Meyers et al. 1991, Hicks et al. 1991, Lovett 1994, Schmitt et al. 2005). There are currently over 70 Clean Air Status and Trends Network (CASNET) sites across the United States monitoring dry deposition, only 27 of which are located in montane landscapes (Baumgardner et al. 2002 and Holland et al. 2004).

In montane forests, throughfall collectors (e.g., open funnel collectors established beneath a forest canopy) measure chemical fluxes from the forest canopy to the forest floor (Clark et al. 1998, Nadkarni 1986). Total deposition (wet + fog + dry) can be estimated with the use of chemical tracers (i.e., conservative elements such as sulfur and chloride). Plants absorb little sulfur and chloride through leaf surfaces and nearly all sulfur and chloride deposited to a canopy passes through in throughfall (i.e., water that drips from the forest canopy) (Lindberg and Garten 1988, Lindberg et al. 1992). For labile nutrients (e.g., nitrogen), foliar uptake (i.e., absorption of nutrients through canopy surfaces) and leaching (i.e., removal of nutrients from

leaves) can be important. Though these nutrients cannot be used as indicators of total deposition, they provide an estimate of total throughfall inputs to the forest floor.

In remote montane areas, bulk and throughfall collection over long periods can be resource demanding, because frequent sampling is required. Ion-exchange resin (IER) collectors offer certain benefits over traditional aqueous collection methods. IER collectors do not need to be replaced as frequently as aqueous samples and can remain in remote areas for weeks to a few months at a time. Though IER sampling periods are reduced in highly polluted systems, due to limited column capacity, IER collectors are useful for measuring atmospheric deposition fluxes in low to moderately polluted systems (Simkin et al. 2004).

## Modeling Deposition in Montane Landscapes

Small-scale heterogeneity in montane environments creates challenges when extrapolating point estimates of atmospheric deposition. Estimates of wet deposition and throughfall can be interpolated over larger spatial scales using empirical models. For example, to improve interpolation of wet deposition data over complex topographies, data collected by the National Atmospheric Deposition Program/ National Trends Network (NADP/NTN) were combined with precipitation data from the Parameter Regression Independent Slope Model (PRISM) (Latysh and Weatherbee 2012, and Nanus et al. 2012). By incorporating landscape variables such as elevation, slope, and aspect, wet deposition can be more accurately represented across complex landscapes.

Though this method is useful for mapping estimates of wet deposition at large scales, mapping total deposition is difficult, because dry deposition estimates are still limited in heterogeneous areas. Weathers et al. (2006b) used extensive throughfall measurements,

satellite imagery, and a Geographic Information System (GIS) to estimate total deposition across the Great Smoky Mountains National Park (GRSM). They found large uncertainties in deposition patterns, which they attributed to small-scale changes in terrain over short distances not captured by satellite images. Overall, modeling atmospheric deposition in montane ecosystems will require a better understanding and means of quantifying small scale meteorological, vegetation, and topographic controls on rates of dry and fog deposition.

## Conclusion

Atmospheric deposition is an important source of nutrients and pollutants to terrestrial and aquatic ecosystems (Fenn et al. 2010, Fowler et al. 1984). Studies in the United States have identified montane forest ecosystems as susceptible to increased rates of atmospheric deposition (Porter et al. 2005, Pickering et al. 2008). The heterogeneity of these ecosystems requires an understanding of how terrain characteristics across large and small scales interact to influence rates of deposition. Current models are useful for estimating atmospheric deposition over flat homogenous landscapes, where there is little change in terrain characteristics. However, in complex high-elevation landscapes, estimates are inaccurate, because data are limited (Latysh and Weatherbee 2012, Nanus et al. 2012). Because dry and fog deposition can vary with micro-scale meteorological patterns and terrain features, it is vital that we accurately assess contributions of dry and fog deposition to total deposition in heterogeneous environments and include these small scale contributions in meso- and large-scale empirical models to improve mitigation strategies and protect ecosystem resources.

TABLE 1. A description of factors influencing atmospheric deposition rates at different spatial scales in montane landscapes.

| Description | References |
|---|---|
| Large Scale (>1000km): Total Deposition (Wet, Fog, and Dry Deposition) | |
| Climate:<br>Atmospheric wet, fog, and dry deposition vary with climate. Near the coast and at high elevations, increased rainfall, fog immersion, and strong winds increase atmospheric deposition. In arid climates and during dry seasons, dry deposition increases relative to wet deposition, whereas in tropical regions and during wet seasons wet deposition increases relative to dry deposition. | Fenn et al. 2003, Holland et al. 2005, Prada et al. 2009, Weathers et al. 2000, Lovett 1994 |
| Elevation:<br>Amount and variability of atmospheric wet, fog, and dry deposition increase with increasing elevation, because of orographic precipitation, fog immersion, and strong winds. | Bradford et al. 2010, Lindberg and Lovett 1992 |
| Proximity:<br>Atmospheric wet, fog, and dry deposition increase with proximity to natural and anthropogenic emission sources. This factor can also affect deposition rates at meso- and micro- scales. | Cape et al. 2008, Chang et al. 2006 |
| Vegetation:<br>In forest ecosystems, atmospheric dry and fog deposition increases with increased canopy cover due to scavenging of gasses and particles by tree leaves, stems, and epiphytes. | Catriona et al. 2012 Ewing et al. 2009, Levia and Frost 2006, |
| Meso-scale (10-1000km) to Small-scale (<10km): Wet, Dry, and Fog Deposition | |
| Edge effect :<br>Atmospheric dry and fog deposition increases with proximity to forest edges or canopy gaps. | Lindberg and Owens 1993, Schrijver et al. 2007 |
| Wind:<br>Atmospheric dry and fog deposition increases with increasing wind speeds. Changes in wind direction can also control distribution and accumulation of particles and gases to canopy surfaces. | García-Santos and Bruijnzeel 2010, Jackson and Hunt 1975 |
| Slope position:<br>Atmospheric dry and fog deposition varies relative to slope position. Ridge tops and steep slopes (e.g., > 20°) along valley walls receive higher deposition than valley floors and flat slopes. | Makowski Gianonni et al. 2013, Schmiss et al. 2011 |
| Small-Scale(<10km): Dry and Fog Deposition | |
| Canopy Exposure :<br>Atmospheric dry and fog deposition increases with canopy exposure relative to surrounding vegetation and topographic relief (e.g., slope curvature). For example, trees along small rises receive more deposition compared to trees along small depressions. | Almquist et al. 2002, Hesp et al. 2013, Weathers et al. 2006b, |
| Canopy Structure:<br>Atmospheric dry and fog deposition increases with increased canopy surface roughness. This can be influenced by difference in canopy height, density, and LAI. | Levia and Frost 2006, Maurer et al. 2013 |

# CHAPTER 2

# EFFECTS OF VEGETATION STRUCTURE AND CANOPY EXPOSURE ON SMALL-SCALE PATTERNS OF ATMOSPHERIC DEPOSITION

## Introduction

Atmospheric deposition is an important component of biogeochemical cycling in forest ecosystems (Fenn et al. 2010, Fowler et al. 1984, Lovett 1994, Weathers et al. 1998, Weathers and Ponette-González 2011). Nutrients and pollutants are deposited to the forest canopy via wet, fog, and dry deposition (Lovett 1994). Ions in the atmosphere that dissolve in water droplets are deposited to vegetation in rain, sleet, and snow (i.e., wet deposition) and fog (i.e., fog deposition). Particles and gases may also settle directly on vegetation surfaces as dry deposition. Total deposition of nutrients and pollutants to the forest canopy is the sum of wet, fog, and dry inputs. Once deposited to the forest canopy, some ions can be readily absorbed by leaves and epiphytes (i.e., canopy uptake) or leached from the canopy (i.e., canopy leaching; Clark et al. 1998, Nadkarni 1986). Some dry particles and gases that are deposited may accumulate on canopy surfaces. Once dissolved in water, these particles and gases are washed from the canopy and delivered to the forest floor in throughfall (i.e., water that drips from the forest canopy to the forest floor). Because of dry and fog deposition, canopy uptake, and canopy leaching, the chemistry of throughfall differs from that of rainfall (Weathers et al. 1998).

Rates of atmospheric deposition vary spatially across terrestrial landscapes (Weathers et al. 2001, Weathers et al. 2006a). Montane environments, in particular, are areas where atmospheric deposition can exhibit high spatial variability at small (<10km) and large spatial scales, because climate, topography, and vegetation vary over short distances (Weathers

et al. 2006b). Studies have shown that compared to low elevation sites, ecosystems at high elevations receive higher amounts of wet deposition due to increased orographic precipitation (Lindberg and Lovett 1992, Weathers et al. 2000). Fog deposition is greater in areas with higher fog frequency such as in montane forest ecosystems (Weathers et al. 2006b). Because fog droplets and particles in the atmosphere are transported via wind, higher wind speeds increase dry and fog deposition to forest canopies exposed to prevailing winds (Lindberg an Lovett 1992). Characteristics of vegetation strongly influence the interception of particles, gases, and fog droplets to montane forests (Ponette-González et al. 2010, Weathers et al. 2006b). For example, evergreen conifer tree species exhibit higher dry and fog inputs compared to broadleaf deciduous tree species because of year-round canopy cover and high leaf area (Weathers et al. 2000).

At smaller spatial scales, studies suggest that differences in atmospheric deposition rates are related to differences in vegetation structure as well as canopy exposure (Weathers et al. 2006b). In mountainous landscapes, variations in relief affect the degree to which an individual tree canopy is exposed to the atmosphere. For example, in flat areas, trees located within small surface depressions are more protected from prevailing winds than trees on small rises that emerge above their neighbors. Similarly, trees growing on steep slopes are more exposed than trees growing on gentler slopes (Weathers et al. 2001). Canopy exposure together with tree structural characteristics (e.g., tree height) may interact to create deposition hotspots (Ponette-González et al. 2010).

The overall goal of this study was to better understand small-scale controls on rates of deposition in a heterogeneous montane landscape. Specific objectives were to: (1) measure

total and net $SO_4^{2-}$-S, $Cl^-$, and $NO_3^-$-N fluxes beneath Douglas fir trees; and (2) explore the influence of canopy structure and exposure on total deposition and throughfall fluxes.

## Methods

### *Study Region*

This research was conducted in Soquel Demonstration State Forest (SDSF), Soquel, California (Fig. 4). SDSF is managed under the California Department of Forestry and Fire Protection (CAL Fire). SDSF (37°2'48.65" N, 121°56'13.16" W) is located within Santa Cruz County ~20 km from the Pacific Ocean, 11 km northeast of the City of Santa Cruz, and 32 km south of San Jose (Fig. 4). Covering 1,085 ha of California's coast redwood forest, SDSF ranges in elevation from 152 m to 762 m. SDSF is situated within California's warm-summer Mediterranean climate zone. Summers (May-August) in this climate region are warm and dry, while winters (December-February) are mild and wet.

Average summer temperature in Santa Cruz County is 17.4°C, while mean winter temperature is 10.7°C (NOAA 1996-2012). During the rainy period (October-April), total annual rainfall ranges between ~546 and 1,563 mm, whereas during the dry period (May-October) total annual rainfall ranges between 22 and 350 mm (Linsley, Kraeger, and Associates, Ltd.). Fog is common in the area, usually occurring in the morning and evening hours of the day; it is especially prevalent following the end of the rainy period in April and throughout the summer months (Ewing et al. 2012). Coastal winds blow onshore from the west between February and June and northwest between August and November. Less frequent strong winds, which bring heavy rainstorms, enter from the east in December and northeast in February.

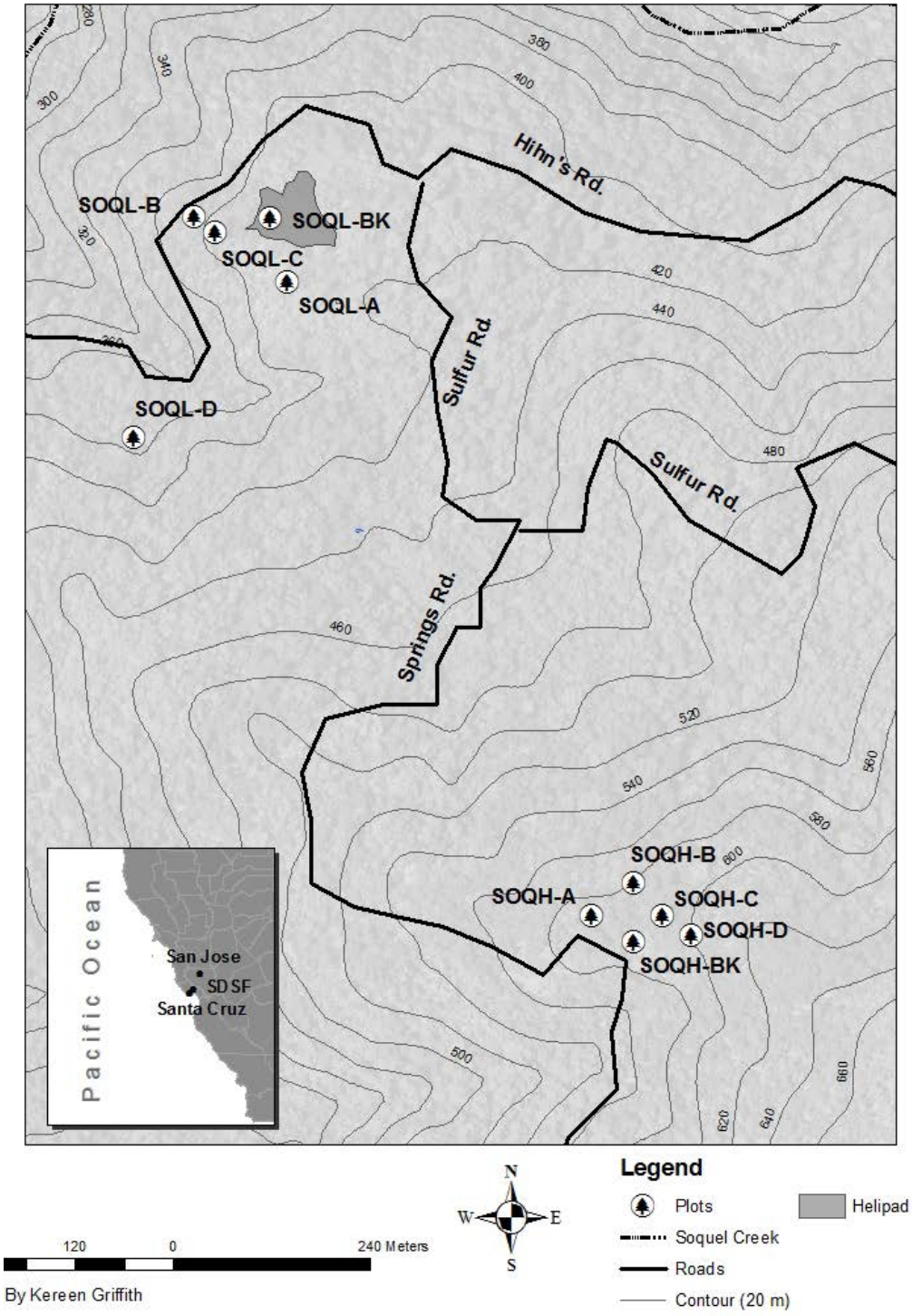


Fig. 4. Map of study region in the Santa Cruz Mountains, California. Two research sites were selected within Soquel Demonstration State Forest (SDSF): the lower helipad (SOQL) and the herpetology study area (SOQH). At each site, four tree clusters (A-D) were selected in the forest and two bulk collectors (BK) were established in adjacent clearings. Difference in elevation between SOQL and SOQH is ~200 m.

SDSF is dominated by two canopy tree species: coast redwood (Sequoia sempervirens) and Douglas fir (Sampson and Orre 2010). At this site, coast redwoods are commonly found in lower valleys running along mountain streams, where they are protected from frequent winds (Noss 1999). Although Douglas fir trees can be found throughout SDSF, they are abundant at low to mid elevations along gentle slopes on southeast and west-facing aspects (Dyrness et al. 1974). Mature Douglas fir trees typically grow to heights of ≥76 m with diameters ~100-110 cm (Hermann et al. 1990).

*Site Selection*

For this study, two sites were selected in SDSF: one near a lower helipad (37°05'22.74" N 121°53'26.75"W, 418 m asl) and one near a herpetology research area (37°04'54.27"N 121°53'09.67"W, 593 m asl; Fig. 1). At each site, a total of four clusters, consisting of three Douglas fir trees each, were selected for a total of eight tree clusters and 24 trees. Tree clusters were chosen using two criteria: canopy exposure and tree size (Table 2). Tree size was determined in the field by measuring tree diameter at breast height (DBH, 1.3 m aboveground). Trees were measured with a DBH tape and then assigned to one of two size classes: intermediate (30-49 cm DBH) or mature (>50 cm DBH). For clusters containing both intermediate and mature trees, average DBH was calculated to determine the appropriate size class.

Clusters of intermediate and mature trees were visually identified as having either an exposed or sheltered canopy. A cluster was identified as exposed when: (1) tree crowns in the cluster emerged above the crowns of neighboring trees; or (2) trees were located on steep upper slopes unsheltered by neighboring trees. All clusters were established on west-facing

slopes to control for aspect, which strongly influences atmospheric deposition (Weathers et al. 2006b), and to ensure that canopies were angled in the direction of the northwest prevailing winds (Table 2). Clusters were established a minimum of 30 m from the helipad, dirt roads, and canopy gaps. Gaps within a forest canopy have been shown to result in increased canopy interception of dry and fog deposition due to increased penetration of fog and wind in the canopy (Lindberg and Owen 1992).

TABLE 2. Description of tree clusters. Clusters at the lower helipad (SOQL) and the herpetology study area (SOQH) were selected based on differences in tree size (intermediate 30-49 cm DBH, mature >50 cm DBH) and canopy exposure. Difference in elevation between sites is ~200 m asl.

| Cluster | Aspect | Exposure | Tree Size | Surrounding Species |
|---|---|---|---|---|
| Site 1: Lower Helipad Site (SOQL) | | | | |
| SOQL-A | 226° | Exposed | Intermediate | Douglas fir and Madrone |
| SOQL-B | 310° | Sheltered | Intermediate | Douglas fir, Madrone, and Live oak |
| SOQL-C | 270° | Exposed | Mature | Douglas fir and Madrone |
| SOQL-D | 332° | Sheltered | Mature | Redwood |
| Bulk | 270° | | | Open |
| Site 2: Herpetology Research Site (SOQH) | | | | |
| SOQH-A | 318° | Exposed | Mature | Douglas fir, Redwood, and Madrone |
| SOGH-B | 308° | Exposed | Intermediate | Douglas fir, Madrone, and Live oak |
| SOQH-C | 328° | Sheltered | Intermediate | Douglas fir and Live oak |
| SOQH-D | 250° | Sheltered | Mature | Douglas fir |
| Bulk | 166° | | | Open |

*Throughfall Fluxes and Bulk Deposition*

In September 2012, a total of 24 ion-exchange resin throughfall collectors were established beneath eight Douglas fir tree clusters in order to measure fluxes of $SO_4^{2-}$, $Cl^-$, and $NO_3^-$ from the canopy to the forest floor (Table 2). Throughfall collection beneath forest canopies is a widely used method for measuring atmospheric inputs to the forest floor in temperate and rainy climates (Weathers et al. 2006b). Sulfur in throughfall can be used to estimate total (wet + fog + dry) atmospheric deposition, because of minimal uptake and

leaching by plant canopies (Lindberg and Lovett 1992). Because nitrogen is a major limiting nutrient that is actively taken up by and leached from plant canopies (Weathers et al. 2006b), total atmospheric deposition cannot be estimated for nitrogen. However, inputs of nitrogen to the forest floor can be determined.

Ion-exchange resins (IER) were used to measure $SO_4^{2-}$, $Cl^-$, and $NO_3^-$ throughfall fluxes. Resin throughfall collectors use small 20 ml chromatograph columns loaded with resin slurry, consisting of ion exchange resin (Dowex Monosphere 550A) and double deionized (DDI) water (Fig. 5). Throughfall collects in the funnel and passes through the ion-exchange resin column, where anions in throughfall adhere to positively charged resin surfaces. Ionic exchange between resins and anions in throughfall prevent $SO_4^{2-}$, $Cl^-$, and $NO_3^-$ in throughfall from passing through the column.

Three throughfall collectors were placed under each tree cluster. Collectors were positioned approximately half way between the trunk and the canopy dripline (i.e., the outer edge of tree crowns) to ensure throughfall and not bulk rainwater was collected. Care was taken to avoid placing collectors close to other collectors or under branches extending outwards from neighboring trees of different species to ensure sampling of Douglas fir throughfall. At each site, two bulk collectors were placed in a nearby open field to estimate bulk deposition of $SO_4^{2-}$, $Cl^-$, and $NO_3^-$ (Table 2). Bulk collectors are open funnels that primarily collect wet deposition (e.g., rainfall), but can also collect a very small amount of dry deposition.

Throughfall and bulk collectors were left open and undisturbed for 8 to 12 weeks during sampling. Samples were collected from 5 October 2012 - 19 December 2012, 20 December 2012 - 22 February 2013, and 23 February 2013 - 25 May 2013 for a total of three collection

periods. After each sampling period ended, funnels were thoroughly rinsed with DI water. IER columns were then removed and replaced with new IER columns. A total of 72 throughfall samples and 12 bulk samples were collected. In addition, a HOBO® data logging rain gauge was also installed at SOQL site adjacent to bulk collectors. Temperature and rainfall were measured at 30-minute intervals from 5 October 2012 - 25 May 2013, to capture climate variability during each sampling period.

Preparation

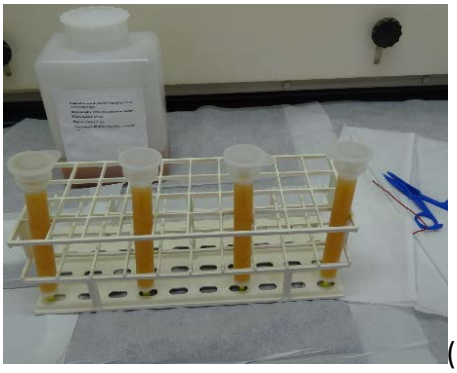

(a)

(b)

Installation

(c)

(d)

FIG. 5. Ion-exchange resin collector preparation and deployment. (a) 20 ml chromatograph columns loaded with anion-exchange resin slurry in the lab. (b) Prepared columns (labeled) and connector pieces (tubing). (c) Installed funnel support for funnel and column. (d) A column containing resin attached to funnel assembly.

*Vegetation Measurements*

Vegetation measurements were obtained for each tree under which a collector was installed. Measurements were conducted in May 2013. DBH measurements were taken with DBH tape and height measurements were taken with a TruPulse® Range Finder. In addition, Leaf Area Index (LAI) readings were taken 1-m from each tree with a LI-COR® LAI- 2200 Plant Canopy Analyzer. Measurements were conducted after sunset during evening twilight (i.e., illumination of sky from sunlight scattering) to prevent interference from direct sunlight passing through the canopy. The LAI sensor was held directly above each collector facing away from the body. The LAI sensor did not touch the rim of the funnel while recording data to avoid contamination of the resin column. For each tree and at the center of each tree cluster, three readings were taken to reduce error. LAI measurements were imported and recomputed from LI-COR® readings following field collection.

*GPS Point Collection*

GPS points were taken directly above throughfall and bulk collectors. A Trimble Geo® 5T handheld device was centered directly above each funnel opening. The GPS device did not touch the rim of the funnel during point collection. At least 40 positions were recorded for each point using both GPS and Global Navigation Satellite System (GLONASS) satellite tracking to improve accuracy. Real-time differential GPS, Wide Area Augmentation System (WAAS), was not used during field collection to ensure post processing of all points. Points taken in the field were post-processed in the lab with GPS Pathfinder® Office. Corrections were based on a correction source, Continuously Operating Reference Station (CORS). UNAVCO, Corralitos, CA (p214) was the closest correction source to study site.

### *LiDAR Point Cloud Data*

LiDAR point cloud data were downloaded from the Open Topography online interface (opentopography.org). The research area within SDSF was identified and delineated with the selection tool available through the Open Topography Google map interface. All sites were within GeoEarthScope's Northern California Airborne LiDAR project coverage area (Dong 2009). These data were downloaded in LASer (LAS) file format. The LAS file was zipped and archived by GeoEarthScope in a tar.gz file (i.e., a compressed archive file) for easy data transfer. Once the LAS file was extracted, an LAS dataset (i.e, storage for LiDAR data and reference feature classes) was created in ArcCatalog.

A 0.5 m resolution digital surface model (DSM) and digital elevation model (DEM) of the study region was created in ArcMap 10.1 from the first (non-ground) and second (ground) return signals classified in the LAS dataset. ArcGIS 10.1 was used to derive a Canopy Height Model (CHM) from differences in DEM and DSM values using the Raster Calculator function available in ArcToolbox. Height displacement between the tree canopy and forest floor (i.e., tree height) was derived from the CHM values. Slope and aspect models were also created with slope and aspect tools available in ArcToolbox. Curvature values were calculated from aggregated DSM (25, 25 m) values. Curvature index values measure the concavity or convexity of the canopy surface relative to surrounding topography and vegetation. Concave depressions are reported as negative values and convex rises are reported as positive values.

### *Sample Analysis*

Ion-exchange resin columns collected in the field were returned to the Ecosystem's Geography laboratory at the University of North Texas (UNT) after each sampling period. Field

samples and blank columns were kept refrigerated throughout the sampling period (October 2012– May 2013). Two blanks were prepared for each sampling period.

Throughfall and bulk samples (n = 84) and sample blanks (n=6) were extracted and diluted following the method of Simkin et al. (2004) and Weathers et al. (2006b). Sulfate, chloride, and nitrate ions collected on resin in columns were extracted with a 1.0 mol/L solution of potassium iodide (KI). Samples were extracted three times for 30 min at 120 rpm using an orbital shaker table. Extractions were diluted at a 3:103 dilution with double deionized water (DDI). Diluted samples were then shipped to Cary Institute's Analytical Laboratory for analysis by ion chromatography. Samples were analyzed on a Dionex™ DX-500 ion chromatograph (IC; Dionex Corporation, Sunnyvale, California, USA) fitted with a Dionex™ Ion-Pac AG9-HC guard column and an AS9-HC analytical column. The detection limit was .02 mg/L.

*Statistical Analysis*

Concentrations (mg/L) reported for $SO_4^{2-}$, $Cl^-$, and $NO_3^-$ were converted to fluxes (kg/ha) per element: (1) by converting to undiluted concentration values based on 3:103 dilution factor; (2) multiplying undiluted concentration values by extracted volume; (3) converting undiluted (mg) values to undiluted (kg) values; and (4) by multiplying undiluted (kg) values by collector surface area (ha). For each collector and sampling period, net throughfall fluxes for $SO_4^{2-}$, $Cl^-$, and $NO_3^-$ were calculated using the following equation:

$$NTF = TF - BD$$

where NTF is net throughfall, TF is throughfall, and BD is bulk deposition (kg/ha). Sulfate in TF was used as an indicator of total atmospheric (wet + dry + fog) deposition and $SO_4^{2-}$ in NTF was used as an indicator of dry and fog deposition. For $NO_3^-$ and $Cl^-$: where NTF > 0, net throughfall

fluxes indicate dry and fog deposition plus foliar leaching, and where NTF < 0, net throughfall fluxes indicate canopy uptake.

Total and net $SO_4^{2-}$, $Cl^-$, and $NO_3^-$ throughfall flux per tree cluster was calculated by taking the average flux of individual collectors in a cluster. Fluxes over the entire 7-month study period equaled the sum of fluxes collected over three sampling periods.

To examine the relationship between vegetation and total and net throughfall fluxes, a simple correlation analysis was used. For individual collectors, a Kolmogorov-Smirnov (K-S) test was used to determine if data were normally distributed. The null hypothesis for the K-S test was not rejected, which confirmed that data collected at SOQL and SOQH were normally distributed for each sampling period. For each sampling period, a Pearson correlation test was run: to examine relationships between total and net $SO_4^{2-}$, $Cl^-$, and $NO_3^-$ throughfall fluxes to individual collectors, variables measured in the field ( e.g., DBH, Height, LAI, and slope), and measurements derived using LiDAR point cloud data (e.g., CHM, slope[a], and curvature). Significant relationships were displayed with scatterplots.

## Results

### *Rainfall and Temperature*

Rainfall measured during the study period (October to May) did not reflect long-term average wet season rainfall in the study region. Total rainfall from October to May was 832 mm, while average wet season rainfall for this region totaled 998 mm. In addition, the rainy period was very wet and relatively short while the dry period was very dry and abnormally long (Fig. 6). Monthly rainfall during November and December was 2-3 times greater than long-term

values (Linsley, Kraeger, and Associates Ltd., 1996-2012), whereas rainfall between January and May was much lower than the long-term values (Fig. 6).

Average monthly temperatures at study site ranged from 7 - 20 °C. Fall temperatures were consistent with long-term averages (NOAA, National Climate Data Center, 1996-2012), whereas winter (December 2012-February 2013) and spring (March 2013-May 2013) temperatures were cooler and warmer than normal (Fig. 6).

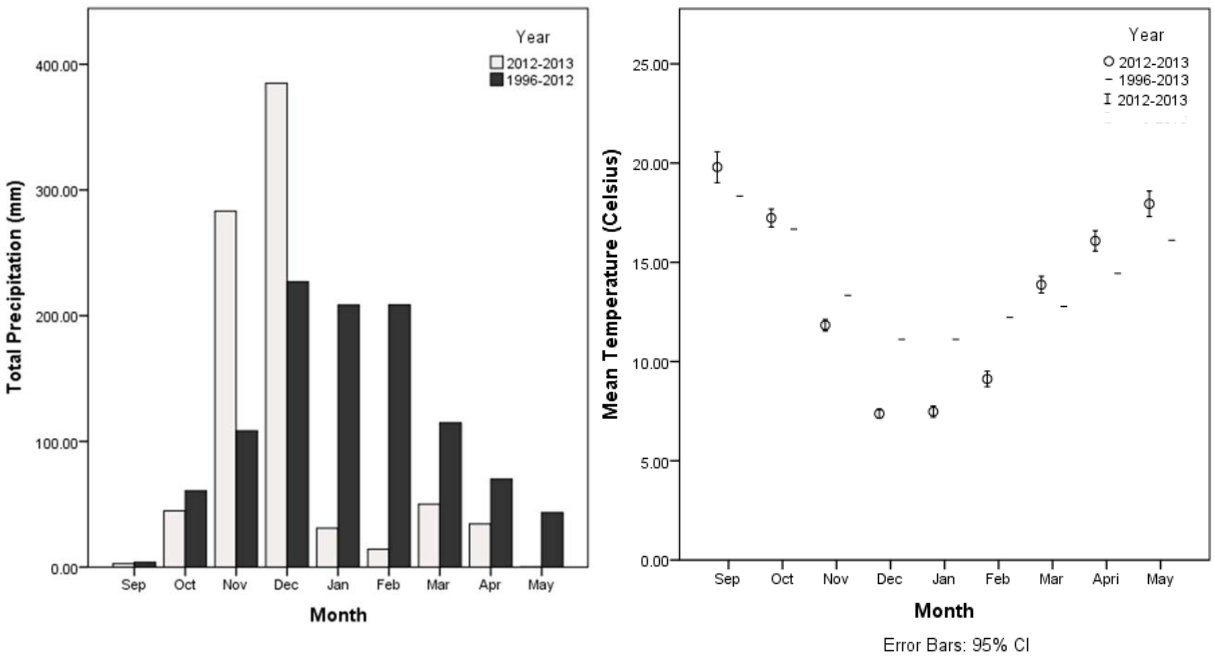


FIG. 6. Climate variability during study period. Monthly rainfall (mm) patterns from 5 October 2012 to 25 May 2013 compared to values for the 1996-2012 period (left). Average monthly temperature (Celsius) patterns from 5 October 2012 to 25 May 2013 recorded in SDSF compared to the 1996-2012 period (right).

*Total Atmospheric Deposition of $SO_4^{2-}$-S*

Total throughfall $SO_4^{2-}$-S fluxes to Douglas fir tree clusters (n=8) ranged from 1.44 - 3.84 kg S $ha^{-1}$ $wet\ season^{-1}$. Total $SO_4^{2-}$-S deposition to exposed/mature clusters was 1.7-2.7 times greater than total $SO_4^{2-}$-S deposition to sheltered and intermediate clusters (Fig. 7).

*Total Throughfall Chloride Fluxes*

Overall, total throughfall fluxes of $Cl^-$ to tree clusters were considerably higher than fluxes of $SO_4^{2-}$-S (Fig. 7). Total throughfall $Cl^-$ fluxes collected ranged from 17.10 – 54.14 kg $Cl^-$ $ha^{-1}$ wet $season^{-1}$. Although $Cl^-$ fluxes were higher than $SO_4^{2-}$-S fluxes, throughfall flux patterns for $Cl^-$ were nearly identical to patterns observed for $SO_4^{2-}$-S (Fig. 7). Like $SO_4^{2-}$-S, total $Cl^-$ fluxes to exposed/mature clusters were substantially higher than fluxes to sheltered and intermediate clusters (Fig. 7). Exposed/mature clusters received 1.5-3.2 times more $Cl^-$ in throughfall compared to other clusters.

*Total Throughfall Nitrate-N Fluxes*

Overall, total throughfall fluxes of $NO_3^-$-N ranged from 0.17 - 4.03 kg N $ha^{-1}$ wet $season^{-1}$. However, total $NO_3^-$-N throughfall fluxes varied between SOQL and SOQH (Fig. 7). Lower $NO_3^-$-N fluxes were observed at SOQL and ranged from 0.17-1.42 kg N $ha^{-1}$ wet $season^{-1}$, whereas higher $NO_3^-$-N fluxes were observed at SOQH and ranged from 1.33 - 4.03 kg N $ha^{-1}$ wet $season^{-1}$. At SOQH, the total $NO_3^-$-N throughfall flux to the exposed/mature cluster was 1.4-3.03 times greater than other clusters. This cluster received higher $NO_3^-$-N than $SO_4^{2-}$-S input (Fig. 7). These patterns were not observed at the lower elevation site.

*Net Throughfall Sulfate-S Fluxes*

Overall, net $SO_4^{2-}$-S throughfall fluxes across clusters ranged from 0.13 -2.37 kg S $ha^{-1}$ wet $season^{-1}$, indicating high variability in dry and fog deposition inputs of sulfur from the canopy to the forest floor. Dry and fog inputs were 9-62% of total $SO_4^{2-}$-S deposition. These inputs were substantially higher for exposed/mature clusters than for other clusters (Fig. 7). Exposed/mature clusters received 2.4-18.2 times more net $SO_4^{2-}$S than sheltered and

intermediate. The highest net throughfall flux was recorded at the exposed/mature cluster at SOQL. Dry and fog deposition to this cluster totaled 2.37 kg S $ha^{-1}$ wet $season^{-1}$, nearly 62% of total deposition and 1.3 -18.2 times more dry and fog deposition than other sites.

*Net Throughfall Chloride Fluxes*

Overall, net throughfall fluxes of $Cl^-$ were all positive and ranged from 3.04 - 39.72 kg $Cl^-$ $ha^{-1}$ wet $season^{-1}$. These fluxes represented 17.8-73.4% of the total chloride measured in throughfall. Differences between total and net throughfall fluxes for $Cl^-$ were slightly greater than differences observed for net $SO_4^{2-}$-S deposition (Fig. 7), suggesting that in addition to dry and fog deposition $Cl^-$ was also leached from the forest canopy. Similar to net $SO_4^{2-}$-S fluxes, net $Cl^-$fluxes to exposed/mature clusters were 2.0-13.1 times higher than other clusters (Fig. 7).

*Net Throughfall Nitrate-N Fluxes*

Net throughfall fluxes for $NO_3^-$-N ranged from (-)1.16 -2.67 kg N $ha^{-1}$ wet $season^{-1}$, indicating net canopy uptake at some sites and net nitrate leaching at others. Similar to total $NO_3^-$-N fluxes, net $NO_3^-$-N fluxes also varied between sites (Fig. 7). Negative net $NO_3^-$-N fluxes were predominantly observed at SOQL and positive net $NO_3^-$-N fluxes was predominantly observed at SOQH (Fig. 7). Net $NO_3^-$-N fluxes were 5.6 - 66.3% of total $NO_3^-$-N throughfall fluxes.

*Small-Scale Variability in Vegetation and Topography*

There was a clear difference in vegetation structure and topographic exposure among tree clusters at SOQL (Table 3). For example, slope angle measured in the field was greater at exposed compared to sheltered clusters (Table 3). Also, elevation (DEM) and digital surface model values (DSM) derived from LiDAR point cloud for exposed clusters were higher than values for sheltered clusters (Table 3). Curvature values were positive at both exposed sites

and negative at both sheltered sites (Table 3). Tree diameter, height, and height (CHM) derived from LiDAR point cloud was greater for mature tree clusters compared to intermediate tree clusters (Table 3). However, for LAI, only one mature tree cluster was greater than intermediate tree clusters (Table 3). Slope, DEM, and DSM were indicators of canopy exposure, whereas DBH, height, and CHM were indicators of tree structure.

There was not a substantial difference between exposed and sheltered clusters at SOQH. Tree DBH, tree height, and CHM were greater at mature clusters compared to intermediate clusters (Table 3). Similar to SOQL, for LAI, only one mature tree cluster was greater than intermediate tree clusters. Slope and slope (slope$^{a}$) derived from LiDAR point cloud were greater at exposed clusters compared to sheltered clusters. However, DEM and DSM measured for exposed clusters were not greater than sheltered clusters (Table 3). Unlike curvature values at SOQL, curvature values at SOQH were not consistently negative at sheltered sites (Table 3). Overall, tree clusters at SOQH differed relative to tree structure, but did not show a substantial difference between clusters relative to canopy exposure.

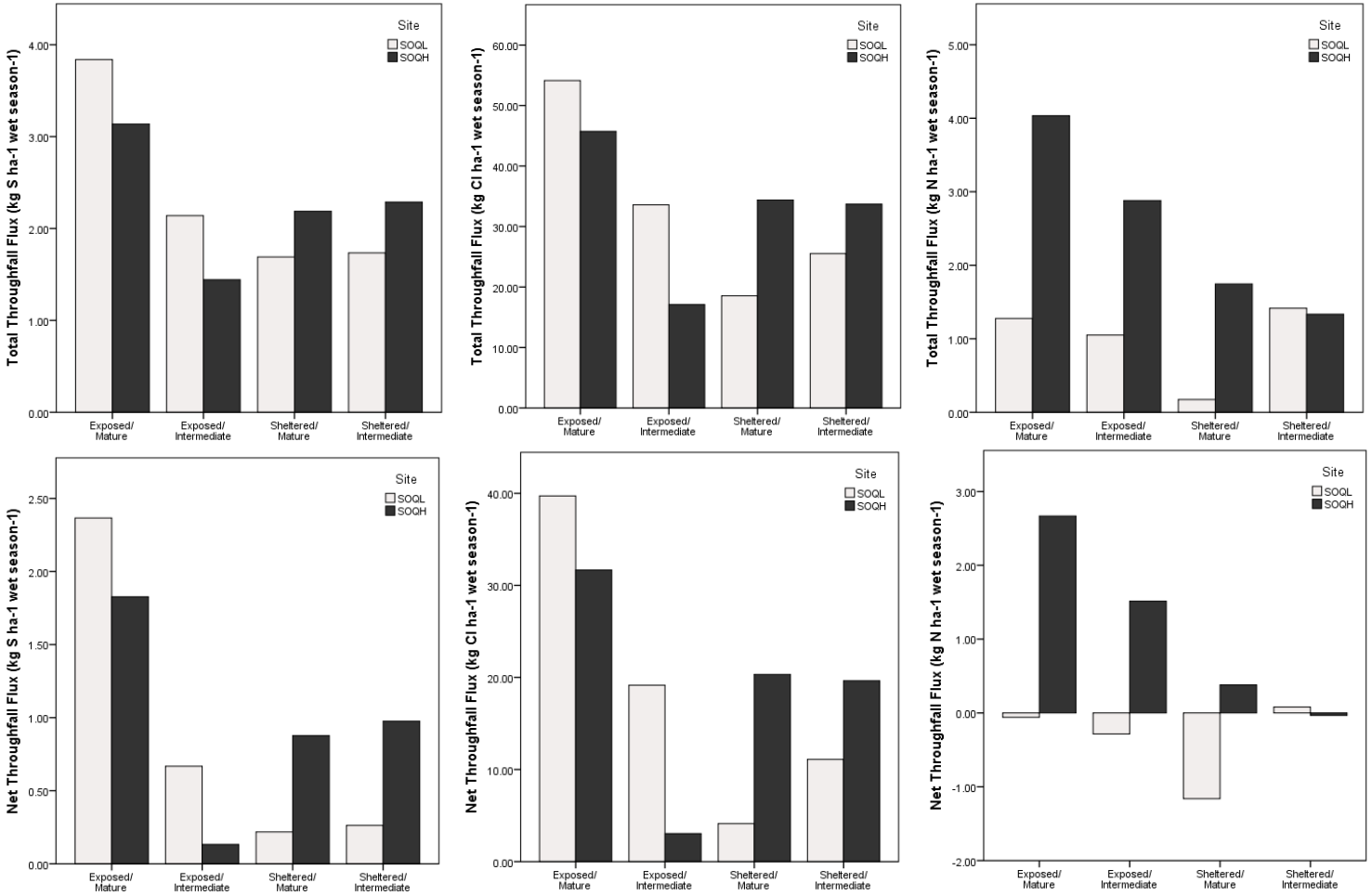


FIG. 7. Total (top) and net (bottom) $SO_4^{2-}$-S, $Cl^-$, and $NO_3^-$-N throughfall fluxes collected from October 2012 – May 2013 under Douglas fir tree clusters (n=8). Total $SO_4^{2-}$-S throughfall fluxes indicate total (wet, fog, and dry) deposition and net $SO_4^{2-}$-S throughfall fluxes indicate inputs from dry and fog deposition. Positive net $Cl^-$ and $NO_3^-$-N through fluxes indicate fog deposition plus dry deposition plus canopy leaching and negative net $Cl^-$ and $NO_3^-$-N throughfall fluxes indicate canopy uptake.

TABLE 3. Summary of vegetation and topographic characteristics for sampled clusters at study sites in Soquel, California.

| | | *Exposed/ Mature* | *Exposed/ Intermediate* | *Sheltered/ Mature* | *Sheltered/ Intermediate* |
|---|---|---|---|---|---|
| *SOQL* | DBH | 121.48 ± 21.83 | 29.83 ± 4.15 | 70.95 ± 23.19 | 43.58 ± 3.43 |
| | Height | 40.87 ± 5.60 | 18.80 ± 0.43 | 46.25 ± 8.98 | 26.73 ± 6.15 |
| | CHM [a] | 36.71 ± 4.55 | 14.85 ± 2.53 | 26.73 ± 7.02 | 22.11 ± 2.45 |
| | LAI | 3.40 ± 0.99 | 3.57 ± 0.12 | 5.64 ± 0.32 | 4.05 ± 0.50 |
| | Slope | 18.83 ± 1.04 | 16.67 ± 2.31 | 10.67 ± 3.06 | 11.50 ± 1.50 |
| | Slope [a] | 19.37 ± 5.05 | 10.56 ± 1.88 | 14.95 ± 1.59 | 10.70 ± 3.96 |
| | DEM [a] | 371.64 ± 1.65 | 388.81 ± 0.97 | 346.07 ± 0.40 | 360.74 ± 0.41 |
| | DSM [a] | 408.35 ± 3.41 | 403.66 ± 3.49 | 372.80 ± 7.32 | 382.86 ± 2.21 |
| | Curvature [a] | 2.54 ± 0.63 | 2.14 ± 0.00 | (-) 2.47 ± 2.04 | (-) 0.08 ± 0.00 |
| *SOQH* | DBH | 79.32 ± 2.35 | 28.55 ± 12.19 | 54.30 ± 23.42 | 33.70 ± 10.43 |
| | Height | 28.43 ± 4.79 | 18.23 ± 5.46 | 28.15 ± 4.01 | 24.77 ± 4.09 |
| | CHM [a] | 21.36 ± 6.70 | 19.48 ± 1.24 | 20.32 ± 2.82 | 15.68 ± 5.00 |
| | LAI | 4.17 ± 0.75 | 3.09 ± 0.79 | 2.99 ± 0.45 | 3.94 ± 0.32 |
| | Slope | 15.00 ± 1.73 | 24.00 ± 4.00 | 3.00 ± 0.50 | 3.33 ± 2.08 |
| | Slope [a] | 13.48 ± 4.52 | 21.46 ± 0.73 | 5.29 ± 2.82 | 4.64 ± 4.41 |
| | DEM [a] | 556.32 ± 0.75 | 553.70 ± 1.04 | 567.40 ± 0.18 | 565.73 ± 0.27 |
| | DSM | 577.68 ± 7.42 | 573.18 ± 2.28 | 587.72 ± 2.97 | 581.21 ± 4.72 |
| | Curvature [a] | 1.70 ± 1.39 | 1.51 ± 0.00 | (-) 1.02 ± 2.66 | 1.57 ± 0.00 |

## Influence of Vegetation Structure and Canopy Exposure on Throughfall

For each sampling period (n=3), a Pearson (r) correlation test was run to assess the relationship between total and net $SO_4^{2-}$-S, $Cl^-$, and $NO_3^-$-N throughfall fluxes to individual collectors and measurements of tree structure and canopy exposure. There were significant positive correlations between: 1) DBH and net $SO_4^{2-}$-S for sampling period 1 ($r = 0.610$, $p < 0.035$), sampling period 2 ($r = 0.461$, $p < .023$), and sampling period 3 ($r = 0.593$, $p < .002$; as well 2) DBH and net $Cl^-$ for sampling period 1 ($r=0.488$, $p < .052$), sampling period 2 ($r=0.488$, $p < .016$), and sampling period 3 ($r = 0.613$, $p < .001$; Table 4). There was also a significant positive correlation between curvature and net $SO_4^{2-}$-S ($r=0.569$, $p < .054$), as well as curvature and net $Cl^-$ ($r = 0.648$, $p < .023$) for sampling period 1 (Table 4). Though there was considerable variability within and between sampling periods, net $SO_4^{2-}$-S and $Cl^-$ tended to increase with increasing DBH and canopy surface convexity (Fig. 8; Fig. 9).

Unlike $SO_4^{2-}$-S and $Cl^-$, total $NO_3^-$-N in throughfall differed between high and low elevation sites (Fig. 10). Elevation at SOQL ranged from 361-372 m, whereas elevation at SOQH ranged from 556-566 m. This suggests that total $NO_3^-$-N throughfall measured at our study site varied with small-scale differences in elevation (184- 205m) or alternatively that this was due to measurement error.

TABLE 4. Pearson (r) correlation coefficients for relationships between total and net throughfall fluxes and vegetation structure and canopy exposure measurements. Twenty-four collectors were sampled for periods 2 and 3. Due to heavy rainstorms and funnel clogging during sampling period 1, throughfall measurements were only available for 12 collectors.

| | Total | | | Net | | | Total | | | Net | | | Total | | | Net | | |
|---|---|---|---|---|---|---|---|---|---|---|---|---|---|---|---|---|---|---|
| | (Period 1) | | | | | | (Period 2) | | | | | | (Period 3) | | | | | |
| | $SO_4^{2-}$-S | $Cl^-$ | $NO_3^-$-N | $SO_4^{2-}$-S | $Cl^-$ | $NO_3^-$-N | $SO_4^{2-}$-S | $Cl^-$ | $NO_3^-$-N | $SO_4^{2-}$-S | $Cl^-$ | $NO_3^-$-N | $SO_4^{2-}$-S | $Cl^-$ | $NO_3^-$-N | $SO_4^{2-}$-S | $Cl^-$ | $NO_3^-$-N |
| DBH | .645* | .571~ | -.185 | .610* | .573~ | -.190 | .490* | .511* | .092 | .461* | .488* | .095 | .564** | .612** | .033 | .593** | .613** | .044 |
| Height | .174 | -.050 | -.365 | .110 | -.053 | -.372 | .124 | .131 | -.245 | .093 | .105 | -.243 | .161 | .166 | -.321 | .197 | .168 | -.308 |
| CHM [a] | .598* | .470 | -.197 | -.552~ | .473 | -.203 | .077 | .077 | .087 | .047 | .053 | .091 | .267 | .338 | .058 | .304 | .340 | .074 |
| LAI | -.480 | -.508~ | -.326 | -.526 | -.506~ | -.329 | -.059 | -.045 | -.278 | -.081 | -.064 | -.276 | -.276 | -.311 | -.212 | -.251 | -.309 | -.200 |
| Slope | .283 | .179 | .382 | .260 | .181 | .375 | .053 | .074 | .116 | .037 | .064 | .118 | -.054 | -.018 | .089 | -.037 | -.017 | .098 |
| Slope [a] | .431 | .196 | .250 | 388 | .198 | .241 | .116 | .116 | -.049 | .099 | .060 | -.048 | .005 | .005 | .035 | .078 | .006 | .044 |
| Curvature [a] | .524~ | .650* | .003 | .569~ | .648* | .008 | .255 | .305 | .216 | .257 | .307 | .217 | .105 | .140 | .105 | .033 | .139 | -.073 |

*[a] LiDAR derived measurement*
*** Significant at the 0.01 level*
** Significant at the 0.05 level*
*~ Significance at the 0.10 level*

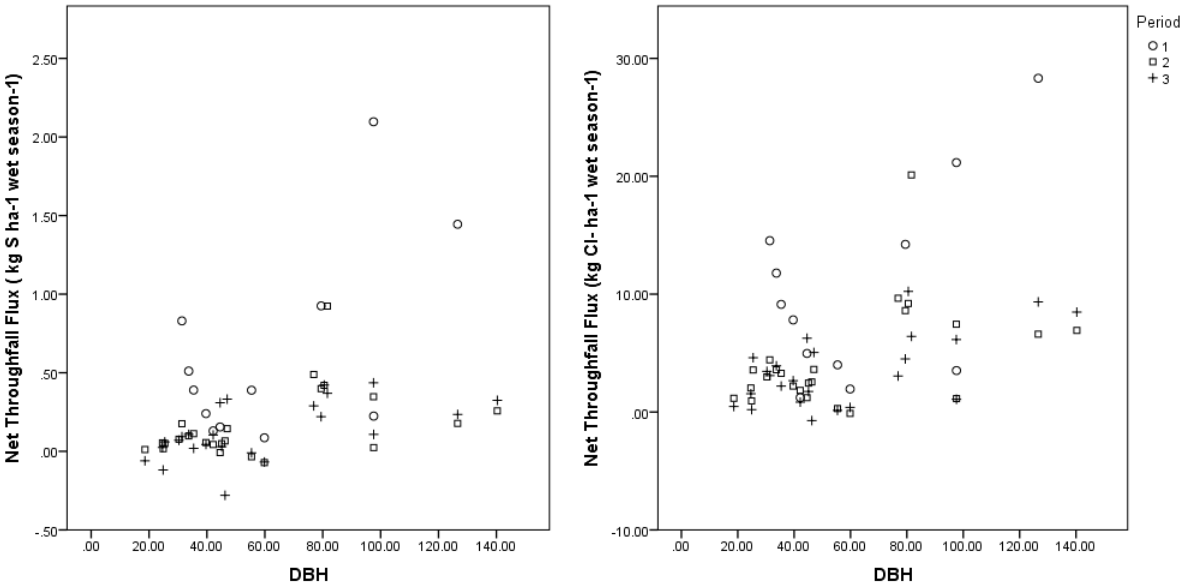


FIG. 8. Scatter plots of tree diameter against net $SO_4^{2-}$-S (left) and net $Cl^-$ (right). Points indicate net throughfall fluxes measured under individual Douglas fir trees during each sampling period. Due to heavy rainstorms and funnel clogging during sampling period 1, net throughfall measurements were only available for 12 collectors.

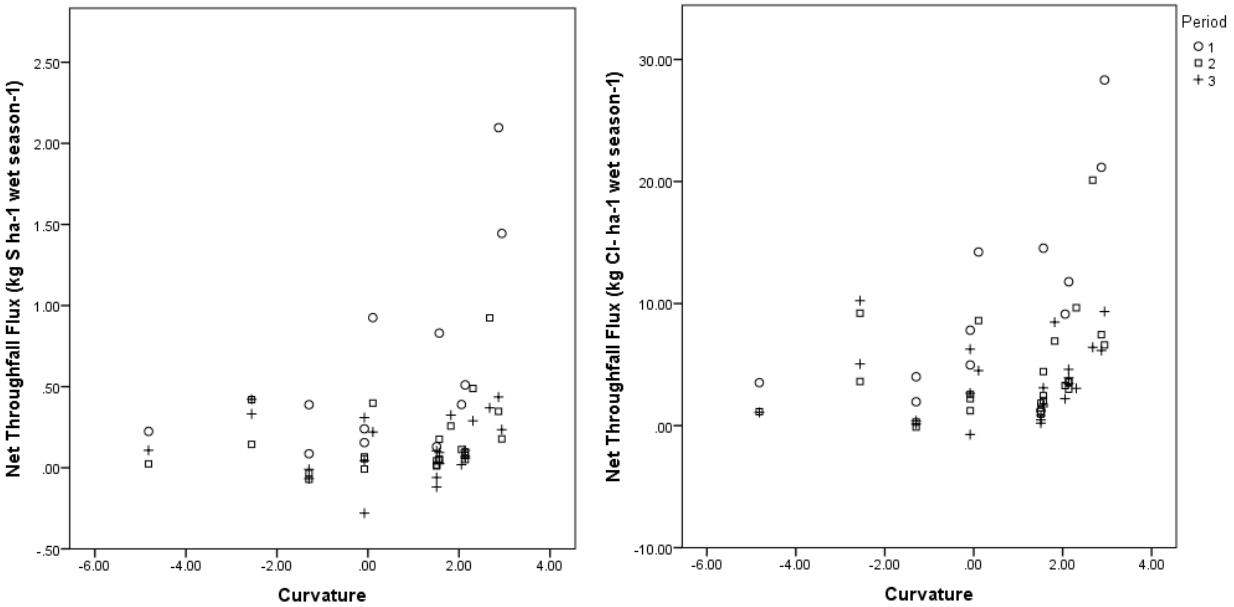


FIG 9. Scatter plots of curvature against net $SO_4^{2-}$-S (left) and net $Cl^-$ (right). Points indicate net throughfall fluxes measured under individual Douglas fir trees during each sampling period. Due to heavy rainstorms and funnel clogging during sampling period 1, net throughfall measurements were only available for 12 collectors.

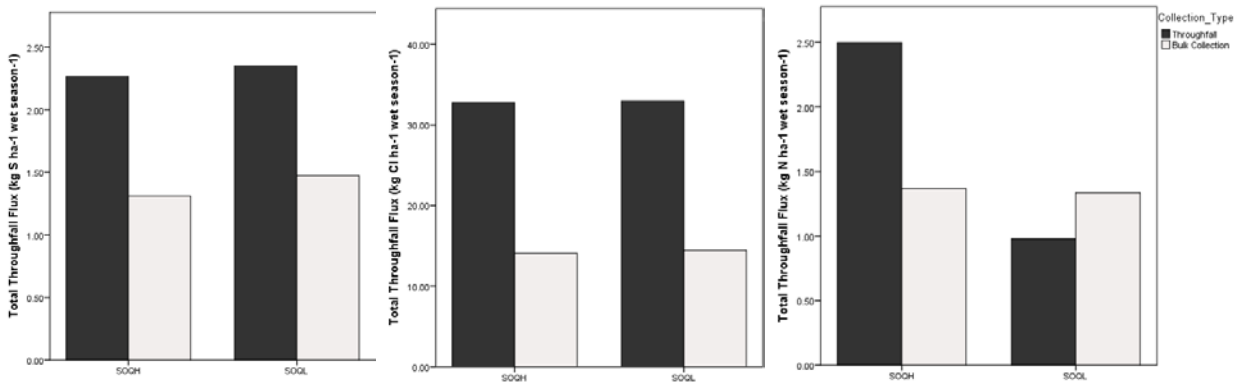


FIG. 10. Total $SO_4^{2-}$-S (left), $Cl^-$ (center), and $NO_3^-$-N (right) throughfall fluxes and bulk deposition at SOQL (lower elevation) and SOQH (higher elevation). Difference in in elevation between SOQL and SOQH is ~200 m.

## Discussion

### *Atmospheric Bulk Deposition*

Wet season bulk deposition measured at SDSF was compared with wet season wet-only deposition measured at NADP/NTN sites in Colorado, California, Washington, North Carolina, and Tennessee (NADP 2012). Molas Pass (CO96) and Niwot Ridge (CO02) are high-elevation sites located in the Colorado Rocky Mountains. Increases in $NO_3^-$-N wet deposition have been observed here since the 1980s (Burns 2004). Olympic National Park (WA14) is situated ~80 km from the ocean along Washington's coast, whereas North Cascades National Park (WA19) is located further inland in north central Washington. Both North Cascades National Park and Olympic National Park are temperate rainforest sites and receive 1561-3023 mm of rainfall annually (Fenn et al. 2013). Yosemite National Park (CA99) is located along Sierra Nevada's west slope, adjacent to the San Joaquin Valley, a center of high agricultural production. Yosemite National Park most resembles the climate zone (e.g., Mediterranean climate zone) of SDSF. Coweeta (NC25) and Great Smokey Mountains National Park (GRSM; TN11) are located along the southern extent of the Appalachian Mountains. In this region, nitrogen oxides ($NO_x$) and sulfur dioxide ($SO_2$) are common pollutants contributing to the occurrence of acid deposition

(Baumgardner et al. 2003). Sources of these pollutants at NC25 and GRSM are primarily from fossil fuel emissions (Driscoll et al. 2001).

Bulk $SO_4^{2-}$-S deposition at SDSF was similar to wet $SO_4^{2-}$-S deposition measured at NC25 and TN11 (Table 5). High levels of sulfate deposition are associated with soil acidification at NC25 and TN11, suggesting that SDSF may be susceptible to soil acidification as a result of high $SO_4^{2-}$-S loads to more exposed areas (Driscoll et al. 2001). At SDSF seasalt sulfate is likely an important source of this ion. Bulk $Cl^-$ deposition at SDSF was 54.1% higher than wet $Cl^-$ measured at WA14 (Table 5). High $Cl^-$ deposition at SDSF can be explained by the area's proximity (~20 km) to the ocean. Nitrate-N deposition at SDSF was 19.9-50.7% lower than wet $NO_3^-$-N fluxes at CO96, CO02, CA99, NC25, TN11, and WA19 (Table 5). Unlike these sites where nitrate deposition is likely influenced by emissions from nearby industrial and agricultural centers (Hedin et al. 1995, McDowell et al. 1990, Weathers et al. 1998), SDSF is not located downwind from agriculture or industry.

*Throughfall Fluxes*

Total and net throughfall fluxes at SDSF were compared to fluxes measured at GRSM, Acadia National Park, and along the Columbia River Gorge (CRG). GRSM and Acadia are located in the eastern United States and experience higher deposition loads due to higher rainfall and higher pollutant emissions (Holland et al. 2005, Lovett 1994). Steep slopes along the CRG frequently funnel emissions from the nearby metropolitan centers of Portland and Vancouver, increasing throughfall fluxes along CRG (Fenn et al. 2007).

Total and net $SO_4^{2-}$-S fluxes at SDSF were lower than total and net $SO_4^{2-}$-S fluxes measured at both GRSM and Acadia (Table 6). For SDSF, the contribution of dry and fog

deposition to total $SO_4^{2-}$-S deposition was 37.4%-42.1%, while at Acadia it was 28.1% - 54.5% and at GRSM it was about 60.0%-72.5%. Although total and net $SO_4^{2-}$-S throughfall fluxes at CRG were much lower than at SDSF, the relatively contribution of dry and fog deposition of $SO_4^{2-}$-S at CRG was more important (72.5% - 84.6%) than at SDSF (Table 6). Weathers et al. (2006b) observed that in the western United States, the relative contribution of dry and fog deposition to total deposition can be comparable to contributions of wet deposition in the eastern United States. Fenn et al. (2013) found that CASTNET estimates of dry deposition, which base dry deposition values on ambient air concentrations in the atmosphere and wind velocity typically underestimate dry deposition, resulting in overall underestimation of total deposition in more arid and heterogeneous landscapes.

Total $Cl^-$ throughfall fluxes measured at SDSF were substantially higher than fluxes measured at Acadia and GRSM (Table 6). Overall chloride fluxes were 6%-69% higher than fluxes measured at sites in the eastern United States. Higher chloride fluxes measured at SDSF can be explained by proximity (~20 km) to the coast and foliar leaching from Douglas fir trees. Grant et al. (2003) found that increased exposure of both lowland and montane areas near the ocean to coastal fog and see spray resulted in higher $Cl^-$ fluxes relative to more inland locations.

Total and net $NO_3^-$-N throughfall fluxes were generally lower than fluxes measured at sites in the eastern United States and CRG. Total $NO_3^-$-N throughfall fluxes at sites in the eastern United States were generally 3-6 times higher than fluxes measured at SDSF, while CRG sites were 6-7 times higher. Net $NO_3^-$-N throughfall fluxes at SDSF ranged from -0.36-1.13 kg N $ha^{-1}$ wet $season^{-1}$, while net throughfall at CRG ranged from 5.7-4.6 kg N $ha^{-1}$ wet $season^{-1}$, and Acadia and GRSM ranged from (-) 0.85-4.00 kg N $ha^{-1}$ wet $season^{-1}$. Fenn et al. (2003) found that

variability in nitrogen emission sources, prevalence of dry and fog N deposition, and landscape heterogeneity in the western United contribute to high variability in N inputs.

Table 5. Wet-only deposition to NADP/NTN network sites and study site locations (SOQL and SOQH) at SDSF from October 2012-May 2013. All sites included are characterized by mountainous terrain.

| Site ID | NADP/NTN Network Sites | Elev. (m) | Ppt. (mm) | $SO_4^{2-}$-S | $Cl^-$ | $NO_3^-$-N |
|---|---|---|---|---|---|---|
| | | | | (kg $ha^{-1}$ wet $season^{-1}$) | | |
| CO96 | Molas Pass | 3248 | 432.5 | 1.22 | 0.44 | 2.78 |
| CO02 | Niwot Saddle | 3520 | 862.6 | 0.71 | 0.24 | 2.09 |
| CA99 | Yosemite National Park | 1393 | 863.5 | 0.67 | 0.76 | 2.53 |
| NC25 | Coweeta | 686 | 1380 | 1.42 | 2.14 | 2.15 |
| TN11 | Great Smokey Mountains National Park | 640 | 1121.1 | 1.44 | 0.50 | 2.37 |
| WA14 | Olympic National Park-Hoh Ranger Station | 182 | 2681.1 | 0.64 | 6.61 | 0.46 |
| WA19 | North Cascades National Park | 124 | 1846.7 | 0.53 | 1.36 | 1.71 |
| SOQH | Herpetology Study Area | 613 | 847 | 1.47 | 14.42 | 1.33 |
| SOQL | Lower Helipad | 418 | 847 | 1.31 | 14.06 | 1.37 |

Table 6. Total throughfall and net throughfall (kg $ha^{-1}$ wet $season^{-1}$) to mountain forest sites along Columbia River Gorge (CRG) in Washington and Oregon, Tennessee( GRSM), Main(Acadia), and study sites at SDSF (SOQH and SOQL) in California. All total and net throughfall reported were collected with IER collectors.

| Site | Elev. (m) | Ppt. (mm) | Total Throughfall $SO_4^{2-}$-S | Total Throughfall $Cl^-$ | Total Throughfall $NO_3^-$-N | Net Throughfall $SO_4^{2-}$-S | Net Throughfall $Cl^-$ | Net Throughfall $NO_3^-$-N | Reference |
|---|---|---|---|---|---|---|---|---|---|
| Acadia | | | | | | | | | |
| Deciduous | 17 - 405 | 1286 | 6.06 | 10.15 | 2.73 | 1.70 | 5.50 | 0.36 | |
| Conifer | | | 9.59 | 22.73 | 4.93 | 5.23 | 18.08 | 2.56 | |
| Mixed Forest | | | 7.85 | 18.89 | 3.17 | 3.50 | 14.24 | 0.79 | |
| GRSM | | | | | | | | | Weathers (unpublished) |
| Deciduous | 700-212 | 450 | 4.79 | 1.98 | 0.94 | (-)0.81 | 0.19 | (-)0.85 | |
| Conifer | | | 40.46 | 10.49 | 5.81 | 34.87 | 8.70 | 4.02 | |
| Mixed Forest | | | 13.91 | 5.52 | 2.73 | 8.32 | 3.72 | 0.95 | |
| CRG | | | | | | | | | |
| Western | 19 - 385 | 253 - 1104 | 1.38 | na | 5.48 | 1.00 | na | 4.60 | Fenn et al. 2007 |
| Eastern | | | 1.88 | na | 6.37 | 1.59 | na | 5.70 | |
| SDSF | | | | | | | | | |
| SOQH | 373 - 565 | 847 | 2.26 | 32.73 | 2.50 | 0.95 | 18.7 | 1.13 | See Results |
| SOQL | | | 2.35 | 32.95 | 0.98 | 0.88 | 18.5 | (-)0.36 | |

*Influence of Vegetation Structure and Canopy Exposure on Throughfall*

Results suggest that $SO_4^{2-}$-S, $Cl^-$, and $NO_3^-$-N throughfall fluxes were influenced by vegetation structure and canopy exposure. First, as an overall measure of total deposition, $SO_4^{2-}$-S fluxes to tree clusters were 1.7-2.7 times higher at exposed/mature tree clusters than at sheltered and intermediate clusters. This pattern was even more pronounced for net $SO_4^{2-}$-S deposition, where exposed/mature tree clusters were 2.4-18.2 times higher than other tree clusters.

Second, DBH was significantly correlated with net $SO_4^{2-}$-S and $Cl^-$ fluxes, indicating that canopy structure did influence rates of dry and fog deposition (Table 4). Other studies have also found correlations between tree height, a significant correlate of DBH, and rates of dry and fog accumulation on leaf, stem, and epiphyte surfaces (Levia and Frost 2006, Maurer et al. 2013). This can be explained by increased surface roughness (Erisman and Draaijers 2003). Although Erisman and Draaijers (2003) identified height and LAI as effective measures of surface roughness, LAI was not significantly correlated with $SO_4^{2-}$-S or $Cl^-$ fluxes at SDSF (Table 5). Similarly, Weathers et al. (2006b) did not find a correlation between $SO_4^{2-}$-S, $Cl^-$, and $NO_3^-$-N throughfall fluxes and LAI. However, dry deposition estimates from leaf wash studies and deposition modeling show that LAI is directly related to nutrient scavenging and accumulation of dry and fog particles to canopy surfaces (Draaijers et al. 1993, Lindberg et al. 1988).

Weathers et al. (2001) noted that increased canopy exposure along steep slopes, ridges, and surface outcrops may account for uncertainties in dry and fog deposition estimates across heterogeneous landscapes. Many of these small-scale surface features are not captured by large-scale deposition monitoring networks (Weathers et al. 2006b). Findings from this study

showed that variability in canopy exposure caused by differences in canopy curvature, may also influence rates of dry and fog deposition (Fig. 9). Increased convexity of canopy surfaces were associated with higher net $Cl^-$ throughfall fluxes. This can be explained by an increase in canopy exposure at these sites relative to sites located along downward concave canopy surfaces. Studies in montane forest ecosystems have attributed high variability in dry and fog deposition to tree height, LAI, and density, but have not quantified effects of canopy surface curvature (Weathers et al. 1992, Weathers et al. 1995, Weathers et al. 2001, Lindberg and Owens 1993).

Although $NO_3^-$-N fluxes did not correlate with vegetation variables, small scale changes in elevation between SOQH and SOQL, just 200 meters, did appear to affect $NO_3^-$-N fluxes (Fig. 10). Higher total and net $NO_3^-$-N throughfall fluxes were observed at higher elevation site at SOQH (Fig. 10). These results are in line with findings reported for other locations in Mt. Orford in Québec, Canada and El Trio mountain pass in southeastern Ecuador that found small-scale changes in elevation along an elevational gradient to significantly influence rates of nitrogen deposition (Markowski Giannoni et al 2013, Lavoie and Bradley).

*Uncertainty*

As a result of funnel clogging due to heavy rainstorms, throughfall measurements were only available for 12 collectors during sampling period 1. Because sample numbers were lower during this period, overall strength of relationships for individual collectors relative to DBH and canopy curvature may have been underestimated.

Accuracy of GPS data gathered for the study site was limited by satellite signal interference during GPS point data collection in the field. Data points collected with Trimble® handheld unit ranged in accuracy from 0.9 -11.0 meters. As a result, it was difficult to identify

precise locations of individual tree canopies on LiDAR derived DEM, DSM, CHM, slope[a], and curvature models. LiDAR measurements for CHM[a] and slope[a] did not strongly correlate with field based measurements of height and slope (Table 7). This suggests that small-scale applications of LiDAR, though accurate, may still be limited by onsite GPS point data collection in areas where large trees and steep slopes interfere with GPS signals.

TABLE 7. A correlation chart for vegetation and topographic measurements taken for individual collectors (n=24) from October 2012-May 2013.

| | DBH | Height | CHM [a] | LAI | Slope | Slope [a] | DEM [a] | DSM [a] | Curvature [a] |
|---|---|---|---|---|---|---|---|---|---|
| DBH | 1 | .709** | .824** | .050 | .257 | .625* | (-).359 | (-).309 | (-).073 |
| Height | .709** | 1 | .637* | .576 | (-).057 | .460 | (-).578* | (-).549 | (-).546* |
| CHM[a] | .824** | .637* | 1 | ..079 | .394 | .667* | (-).450 | (-).390 | (-).004 |
| LAI | .050 | .576 | .079 | 1 | (-).428 | (-).187 | (-).391 | (-).397 | (-).857** |
| Slope | .257 | (-).057 | .394 | (-).428 | 1 | .800** | (-).182 | (-).159 | .348 |
| Slope [a] | .625* | .460 | .667* | (-).187 | .800** | 1 | (-).403 | (-).365 | .020 |
| DEM [a] | (-).359 | (-).578* | (-).450 | (-).391 | (-).182 | (-).403 | 1 | .998** | .379* |
| DSM [a] | (-).309 | (-).549* | (-).390 | (-).397 | (-).159 | (-).365 | .998** | 1 | .391* |
| Curvature [a] | (-).073 | (-).546* | (-).004 | (-).857** | .348 | .020 | .379* | .391* | 1 |

*** Significant at the 0.01 level*
** Significant at the 0.05 level*
*[a] LiDAR derived measurement*

## Conclusion

Mountain forest landscapes provide vital ecosystem services, such as fresh water storage and filtration. However, these ecosystems are also susceptible to increased atmospheric deposition loads. Many of these ecosystems are biodiversity hotspots. Increased inputs from wet, dry, and fog deposition can threaten biodiversity, soil nutrient retention, and water quality of headwater lakes and streams (Bailey et al. 2005, Pardo et al. 2011, Schaberg et al. 2001). In montane forest ecosystems, relative amounts of dry and fog deposition are

important and can be more influential than wet deposition. Further analysis and quantification of small-scale variability in vegetation structure and canopy exposure can improve our understanding of dry and fog deposition and help us improve the accuracy of atmospheric deposition models in heterogeneous landscapes. Advances in high resolution remote sensing tools, such as LiDAR, may help us quantify small-scale variability in vegetation structure and canopy exposure in heterogeneous landscapes, but applications for LiDAR may still be limited by accurate onsite GPS data collection.

Our results confirm that atmospheric deposition and throughfall fluxes did vary with vegetation structure and canopy exposure. Increased deposition of $SO_4^{2-}$-S to exposed/mature tree clusters was predominantly a result of increase dry and fog deposition. For individual tree canopies, fluxes were significantly influenced by differences in DBH and curvature.

# CHAPTER 3

## CONTRIBUTIONS TO THE FIELD OF GEOGRAPHY

Though human geographers predominantly study human activity on earth and physical geographers primarily focus on the natural landscape, both human geographers and physical geographers often explore the consequences of human-environmental interactions (Baerwald 2010). Increasing anthropogenic emissions and atmospheric deposition to terrestrial and aquatic ecosystems is one impact humans have had on the environment. This impact is of interest to human and physical geographers, because of the potential effects on vital ecosystem services (e.g., carbon sequestration, fresh water availability and quality, lumber, food, and recreation; Skole 2004). With advances in geospatial technology and remote sensing, spatial analytical tools are now vital in monitoring local, regional, and global trends in anthropogenic emissions and deposition (Turner et al. 2003 and Boyd 2009).

Although steady increases in deposition to terrestrial and aquatic ecosystems are correlated with increasing anthropogenic emissions, atmospheric deposition and its effects vary with geographic location, time, and scale (Bobbink et al. 2010, Chapin et al. 2012, Schlesinger et al. 2013). This thesis measured atmospheric deposition and throughfall fluxes of $SO_4^{2-}$, $Cl^-$, and $NO_3^-$ to Douglas fir tree clusters in a montane forest in California during an entire rainy season. Montane forest ecosystems receive higher deposition loads, because of higher rainfall, wind speeds, and fog immersion at higher elevations relative to neighboring lowlands (Fowler et al. 1984, Igawa et al. 2001, Lovett 1994, Weathers et al. 2000). However, montane forests are highly heterogeneous and estimating small-scale changes in atmospheric deposition across these landscapes is currently not possible using data from large-scale monitoring networks

(e.g., NADP and CASTNET; Latysh and Wetherbee 2012). These networks lack detailed data on atmospheric deposition and information on small-scale differences in vegetation structure and canopy exposure that control deposition rates in montane forests (Fenn et al. 2013, Weathers et al. 2006b).

The objective of this study was to quantify the effects of vegetation structure and canopy exposure on rates of atmospheric deposition to Douglas fir canopies in a heterogeneous montane forest ecosystem. Small-scale differences in canopy structure and exposure were found to influence rates of dry and fog deposition. Specifically, tree diameter and canopy surface curvature were found to affect $SO_4^{2-}$-S and $Cl^-$ inputs, while elevation may have influenced $NO_3^-$-N fluxes. These finding will contribute to our understanding of small-scale variability in atmospheric deposition and thus help researchers predict where deposition "hotspots" may occur.

Future research on heterogeneity of atmospheric deposition is of interest and can be applied to multiple areas within geography. This research could be used in landscape ecological studies of emerging infectious disease (EID) spread (Meentemeyer et al. 2011); biogeographical studies of changing plant species distributions (McNeill et al. 2007); and ecological disturbance studies focused on mapping changes in vegetation structure and composition in response to changes in natural and anthropogenic disturbances (Turner et al. 2003).

## Modeling spread of Phytophthora ramorum in U.S. Pacific Forests

Phytophthora ramorum is a fungal pathogen that spreads following the release of mobile spores (i.e., propagules) during moist conditions (Rizzo and Garbelotto 2003). These propagules generally travel between 5-10 m, decreasing in number with distance (Davidson et

al. 2005). However, strong winds have been shown to spread infected spores over 100 m (Davidson et al. 2002). Propagules are deposited to host species through atmospheric wet, dry, and fog deposition, and transported by humans (e.g., hiking, biking, and camping) from uninfected to infected areas (Cushman and Meentemeyer 2008, Meentemeyer et al. 2011). Since the 1990s, P. ramorum has rapidly spread, killing millions of tanoaks and oak species along California's west coast (Meentemeyer et al. 2011). Though there is currently no cure or treatment for P. ramorum, current prevention methods focus on controlling direct human interactions (e.g., development of quarantine areas and efforts to clean vehicles and equipment used by hikers, bikers, and field workers), removing infected species, and regulating introduction of infected plant species through timber management (Rizzo and Garbelotto 2003).

The moist climate and number of host species in California forests has contributed to the spread of P. ramorum (Rizzo and Garbelotto 2003). Because of the high virulence of this pathogen, forest managers focus preventative efforts on highly susceptible areas to prevent further spread (Rizzo and Garbelotto 2003). Biogeographers studying plant pathogens currently rely on "pattern-based" approaches to model the spread of emergent diseases (Plantegenest et al. 2007). These models account for effects of moisture, host patterns on the landscape, and elevation (Kelly and Meentemeyer 2002, Plantegenest et al. 2007), but do not include small scale controls on atmospheric deposition (e.g., vegetation structure and canopy exposure), although these are important in controlling propagule deposition. Given the influence of wind driven dry and fog deposition on the spread of propagules in heterogeneous montane landscapes, findings from this study could help to improve pattern-based models of emergent

disease spread. By including small-scale controls on deposition (e.g., DBH and canopy curvature), these models might be able to better pinpoint areas highly susceptible to P. ramorum where preventative measures could be strengthened.

## Effects of nitrogen cycling on plant species composition

In the western United States, increases in nitrogen (N) inputs from atmospheric deposition may have long-term effects on terrestrial biodiversity (Bobbink et al. 2010, Fenn et al. 2003). Although nearly all ecosystems receive some amount of N input from natural sources (background deposition rate is ~0.5 kg N ha $yr^{-}$; Galloway et al. 2008), gradual increases in N deposition are primarily a result of increases in transportation, industry, and agriculture (Fenn et al. 2003, Galloway et al 2004, Schlesinger et al. 2013). Bobbink et al. (2010) reviewed the immediate and long-term effects of increased nitrogen inputs on terrestrial plant biodiversity. These effects include: 1) direct toxicity to individual species resulting in foliar damage; 2) high nitrogen availability leading to changes in plant species interactions in normally nitrogen-limited ecosystems; 3) soil acidification; and 4) increased susceptibility to external environmental stresses, such as disease spread.

In N-limited systems, such as montane forests in California, nitrogen accumulation from increased atmospheric deposition has been shown to promote the spread of nitrogen-limited species and highly tolerant species as well as contribute to the abundance of invasive species (Fenn et al. 2003, Fenn et al. 2008, Geiser et al. 2010). These shifts in plant species interactions due to reduced competition for available nutrients can lead to biodiversity loss (Bobbink et al. 2010, Fenn et al. 2008). Because of increased nitrogen deposition and observed shifts in plant species interactions, Mediterranean forests in California are susceptible to biodiversity loss

(Bobbink et al. 2010, Fenn et al. 2008). Studies in the United States and Europe are also finding that even small increases in nitrogen inputs are contributing to decreased abundance of nitrogen sensitive lichen species (Fenn et al. 2003, Geiser et al. 2010). In California, Fenn et al. (2008) observed changes in lichen communities from sensitive to more tolerant species at ~3 kg N $ha^{-1}$ $yr^{-1}$, while McCune et al. (2007) observed local extinction of highly nitrogen sensitive species at ~6 kg N $ha^{-1}$ $yr^{-1}$.

Though soils in California forests are basic and generally well buffered against acid deposition, highly polluted areas (greater than 10 kg N $ha^{-1}$ $yr^{-1}$) in southern California do experience soil acidification (Fenn et al. 2008). In these areas, soil acidification and nutrient enrichment may contribute to changes in understory plant communities. In the San Bernardino Mountains, just east of Los Angeles, continued anthropogenic disturbance, lack of rainfall, soil acidification, nutrient enrichment, and abundance of invasive species led to a 20-30 % loss of native plant species from 1973-2003 (Allen et al. 2007). Nitrogen accumulation and increased litterfall in the San Bernardino Mountains has been linked to the establishment of the European Gallium aparine, which naturally thrives in thick litter layers and acidified nitrogen-rich soils (Bobbink et al. 2010, Takemoto et al. 2001). Changes such as these in the forest understory can have long-term implications for ecological succession and plant species distributions.

Because of the long term effects of increased nitrogen deposition on plant species composition and landscape patterns, consequences of nutrient enrichment in susceptible ecosystems should be important to both ecologists as well as Biogeographers. Accurate representation of areas of high atmospheric deposition is necessary for determining accurate nutrient load and critical load limits in vulnerable ecosystems.

## Geographer's Toolbox

Geographers possess a unique toolset of geospatial technologies that continue to expand the boundaries of data acquisition and analysis (Table 8). Many of these tools are applied outside the discipline of geography. LiDAR is a newer remote sensing technology that has growing appeal in many different disciplines. In addition to remote sensing technologies, geographers also inherently consider effects of scale, which is important for understanding and predicting regional and global trends in anthropogenic emissions and subsequent effects of increased atmospheric deposition on terrestrial and aquatic ecosystems.

### *Applications of LiDAR in Forestry*

Light detection and ranging, or LiDAR, is a new geospatial technology gaining widespread use in local forestry research, management, and planning (Akay et al. 2007). The successful use of LiDAR in forest science is a result of its unique ability to map vertical and horizontal landscape variability with high accuracy and resolution (Lim et al 2003; Table 8). LiDAR actively captures the vertical and horizontal distribution of features on Earth's surface (Lim et al 2003; Table 8). This is important for mapping attributes of forest structure in montane forest landscapes. Sub-canopy topography, canopy height, and vertical distribution of intercepted surfaces can be derived directly from multipoint return and full-waveform LiDAR sensors (Akay et al. 2007). These parameters are then used to model biomass, volume, and density of vegetation within a forest (vital contributors to P. ramorum spread and the development of atmospheric deposition hotspots). Parameters are processed using gridded digital rasters, where each cell represents quantified attributes of vertical canopy structure (Akay et al. 2007, Lim et al 2003). Once data are processed and converted into gridded raster's

for analysis, surface roughness, canopy exposure, and vegetation structure can be easily calculated. Further geostatistical analysis (e.g., spatial autocorrelation and regression analysis) are also easily run in Geographic Information Systems (GIS).

Improvements in remote sensing technologies in the last decade are attributed to equivalent advances in global positioning systems (GPS), inertial navigational systems, (INS) and inertial measurements units (IMU) (Lim et al 2003). These improvements have increased the applicability of remote sensing tools like LiDAR for mapping vegetation structure and canopy exposure at small spatial scales. For high resolution analysis of small scale characteristics of forest structure, studies have tested the effectiveness of LiDAR at modeling three dimensional characteristics of individual tree crowns (Dong 2009, Osada 2002). LiDAR data for SDSF were used to examine the influence of vegetation structure and canopy exposure on atmospheric deposition and throughfall ion fluxes for small clusters and individual Douglas fir trees. Though the strength of the results were reduced due to uncertainties associated with sampling and onsite GPS point data collection, the findings of this thesis confirmed that changes in vegetation structure and canopy exposure have important effects on deposition rates in heterogeneous ecosystems. Continued push for the application of large-footprint LiDAR scanners in forestry has led to comparative studies across multiple regions (Korhonen et al. 2011). Although these studies have successfully shown LiDAR's accuracy and applicability for plot delineation of forest structure, LiDAR is still not widely available for use in most parts of the world (Lim et al 2003).

TABLE 8. Common remote sensing technologies and associated applications. LiDAR is an active sensor capable of gathering three-dimensional terrain and canopy data based on high-resolution digital elevation models (DEM) and digital surface models (DSM). Data collected at higher resolutions allow for detailed small-scale analysis of vegetation structure (e.g., tree height).

| Sensor | Spatial Resolution | Temporal Resolution | Swath Width | Sensor Type | Application |
|---|---|---|---|---|---|
| | Image Detail | Orbit Cycle/ Revisit Period | Coverage | | |
| LiDAR | < 0.5m | 1-2 day(s) | varies | Active | small-scale 3D terrain mapping (DEM and DSM) |
| GEOEYE -1 | 1.65 m | 24 hr | 590 km | Passive | large-scale high resolution satellite imaging (defense and disaster relief) |
| SPOT 5 | 2.5 m | 2-3 days | 60 km | Passive | Medium-scale high resolution imaging(land use land cover change since 2002) |
| LAND-SAT TM | 30 m | 16 days | 185 km | Passive | medium resolution multispectral imaging (land use land cover change since 1999) |
| NOAA ANHRR | 1100 m | 12 hr | 2000 km | Active | Large-scale low resolution terrain mapping (DEM) |

*Scale*

Consideration of spatial scale is also vital when studying atmospheric deposition in heterogeneous landscapes (Sayre 2005). Scale is a foundational concept in geography. Both geographers and ecologists utilize scale methodologically (e.g., determining relative size of study area for analysis), ontologically (e.g., scale based on size of subject matter), and thematically (e.g., analysis of functions within a certain boundary) to differentiate levels of detail for analysis and determining the extent of key surface features. However, geographers are often better equipped to both quantify and visually represent features on Earth based on relational and conditional interactions across spatial scales (Herod 2010). This approach to scale is a vital tool for not just interpreting and quantifying dynamic interactions (i.e., elements

driving wind and determining surface roughness) within a heterogeneous system, but also for scaling up these phenomena to regional or even global scales (Sayre 2005).

## Conclusion

Since the 1980s, documented increases in anthropogenic emissions have enhanced deposition loads to terrestrial and aquatic ecosystems (Grant et al 2003, Matson 2002). Many ecosystems, including montane forests in California, have already been affected by these increases (Fenn et al. 2008, Menz and Seip 2004). Current research focuses on long-term implications of deposition on vital ecosystem services and biodiversity loss in vulnerable areas, such as SDSF. Many of these areas, susceptible to environmental stresses from nitrogen enrichment and acidification, are already threatened by the spread non- native insects, plant species, and disease (Lovett et al. 2013). Geographers not only contribute vital tools to improve our understanding of small scale meteorological and land surface interactions in heterogeneous ecosystems, but can also benefit from a better understanding of how humans have and will continue to impact natural environments on earth, both locally as well as globally.

REFERENCES

Adon, M., Galy-Lacaux, C., Yoboue, V., Delon, C., Solmon, F., & Kaptue Tchuente, A. T. 2013. Dry deposition of nitrogen compounds (NO 2, HNO 3, NH 3), sulfur dioxide and ozone in West and Central African ecosystems using the inferential method. Atmospheric Chemistry and Physics Discussions 13: 11689-11744.

Akay, A. E., Oğuz, H., Karas, I. R., & Aruga, K. 2009. Using LiDAR technology in forestry activities. Environmental Monitoring and Assessment 151:117-125.

Allen Edith, B., Temple Patrick, J., Bytnerowicz Andrzej, A. M. J., Sirulnik Abby, G., & Rao Leela, E. 2007. Patterns of understory diversity in mixed coniferous forests of southern California impacted by air pollution. The Scientific World Journal 7:247-263.

Almquist, E., Jack, S. B., and Messina, M. G. 2002. Variation of the treefall gap regime in a bottomland hardwood forest: relationships with microtopography. Forest Ecology and Management 157:155-163.

Baerwald, T. J. 2010. Prospects for geography as an interdisciplinary discipline. Annals of the Association of American Geographers 100: 493-501.

Bailey, S. W., Horsley, S. B., & Long, R. P. 2005. Thirty years of change in forest soils of the Allegheny Plateau, Pennsylvania. Soil Science Society of America Journal 69:681-690.

Balestrini, R., & Tagliaferri, A. 2001. Atmospheric deposition and canopy exchange processes in alpine forest ecosystems (northern Italy). Atmospheric Environment 35:6421-6433.

Baumgardner Jr, R. E., Isil, S. S., Lavery, T. F., Rogers, C. M., & Mohnen, V. A. 2003. Estimates of

cloud water deposition at mountain acid deposition program sites in the Appalachian Mountains. Journal of the Air & Waste Management Association. 53: 291-308.in alpine forest ecosystems (northern Italy). Atmospheric Environment 35:6421-6433.

Baumgardner, R. E., Lavery, T. F., Rogers, C. M., & Isil, S. S. 2002. Estimates of the atmospheric deposition of sulfur and nitrogen species: Clean Air Status and Trends Network, 1990-2000. Environmental Science & Technology 36: 2614-2629.

Bobbink, R., Hicks, K., Galloway, J., Spranger, T., Alkemade, R., Ashmore, M., ... & De Vries, W. 2010. Global assessment of nitrogen deposition effects on terrestrial plant diversity: a synthesis. Ecological Applications 20: 30-59.

Bohrer, G., Katul, G. G., Walko, R. L., and Avissar, R. 2009. Exploring the effects of microscale structural heterogeneity of forest canopies using large-eddy simulations. Boundary-Layer Meteorology 132:351-382.

Bradford, D. F., Stanley, K., McConnell, L. L., Tallent-Halsell, N. G., Nash, M. S., and Simonich, S. M. 2010. Spatial patterns of atmospherically deposited organic contaminants at high elevation in the southern Sierra Nevada Mountains, California, USA. Environmental Toxicology and Chemistry 29:1056-1066.

Boyd, D. S. 2009. Remote sensing in physical geography: a twenty-first century perspective. Progress in Physical Geography 33: 451-456.

Burns, D. A. 2003. Atmospheric nitrogen deposition in the Rocky Mountains of Colorado and Southern Wyoming—a review and new analysis of past study results. Atmospheric Environment 37: 921-932.

Caldwell, C. A., Swartzendruber, P., & Prestbo, E. 2006. Concentration and dry deposition of

mercury species in arid south central New Mexico. 2001-2002. Environmental Science & Technology 40: 7535-7540.

Clarkson, D. T., & Hanson, J. B. 1980. The mineral nutrition of higher plants. Annual review of plant physiology 31: 239-298.

Chang, S. C., Yeh, C. F., Wu, M. J., Hsia, Y. J., and Wu, J. T. 2006. Quantifying fog water deposition by in situ exposure experiments in a mountainous coniferous forest in Taiwan. Forest Ecology and Management 224: 11-18.

Chapin III, F. S., Matson, P. A., & Vitousek, P. M. 2012. Nutrient Cycling. InPrinciples of Terrestrial Ecosystem Ecology (pp. 259-296). Springer New York.

Chapman, L. 2000. Assessing topographic exposure. Meteorological Applications 7: 335-340.

Clark, K. L., N. M. Nadkarni, D. Schaefer, and H. L. Gholz. 1998. Atmospheric Deposition and Net Retention of Ions by the Canopy in a Tropical Montane Forest, Monteverde, Costa Rica. Journal of Tropical Ecology 14: 27-45.

Cushman, J., & Meentemeyer, R. K. 2008. Multi-scale patterns of human activity and the incidence of an exotic forest pathogen. Journal of Ecology 96: 766-776.

Daly, C., Halbleib, M., Smith, J. I., Gibson, W. P., Doggett, M. K., Taylor, G. H., and Pasteris, P. P. 2008. Physiographically sensitive mapping of climatological temperature and precipitation across the conterminous United States. International Journal of Climatology 28: 2031-2064.

Davidson, J. M., Rizzo, D. M., Garbelotto, M., Tjosvold, S., & Slaughter, G. W. 2002.

Phytophthora ramorum and sudden oak death in California: II. Transmission and survival. In Standiford, RB; McCreary, D.; and Purcell, KL, technical coordinators. Proceedings of the fifth symposium on oak woodlands: oaks in California's changing landscape. Gen. Tech. Rep. PSW-GTR-184, Albany, CA: US Department of Agriculture, Forest Service, Pacific Southwest Research Station 741-749.

Davidson, J. M., Wickland, A. C., Patterson, H. A., Falk, K. R., & Rizzo, D. M. 2005. Transmission of Phytophthora ramorum in mixed-evergreen forest in California. Phytopathology 95: 587-596.

Dong, P. (2009). Characterization of individual tree crowns using three-dimensional shape signatures derived from LiDAR data. International journal of remote sensing 30: 6621-6628.

Duarte, N., Pardo, L. H., & Robin-Abbott, M. J. 2013. Susceptibility of forests in the northeastern USA to nitrogen and sulfur deposition: critical load exceedance and forest health. Water, Air, & Soil Pollution 224: 1-21.

Driscoll, C. T., Lawrence, G. B., Bulger, A. J., Butler, T. J., Cronan, C. S., Eagar, C., ... & Weathers, K. C. 2001. Acidic Deposition in the Northeastern United States: Sources and Inputs, Ecosystem Effects, and Management Strategies The effects of acidic deposition in the northeastern United States include the acidification of soil and water, which stresses terrestrial and aquatic biota. BioScience *51*:180-198.

Erisman, J. W., and Draaijers, G. 2003. Deposition to forests in Europe: most important factors influencing dry deposition and models used for generalization. Environmental Pollution 124: 379-388.

Ewing, H. A., Weathers, K. C., Templer, P. H., Dawson, T. E., Firestone, M. K., Elliott, A. M., and Boukili, V. K. 2009. Fog water and ecosystem function: heterogeneity in a California redwood forest. Ecosystems 12: 417-433.

Fenn, M. E., E. B. Allen, S. B. Weiss, S. Jovan, L. H. Geiser, G. S. Tonnesen, R.F. Johnson, L.E. Rao, B. S. Gimeno, F. Yuan. T. Mexiner, and A. Bytnerowicz. 2010. Nitrogen Critical Loads and Management Alternatives for N-impacted Ecosystems in California. Journal of Environmental Management 91: 2404–2423.

Fenn, M. E., Geiser, L., Bachman, R., Blubaugh, T. J., & Bytnerowicz, A. 2007. Atmospheric deposition inputs and effects on lichen chemistry and indicator species in the Columbia River Gorge, USA. Environmental pollution 146: 77-91.

Fenn, M. E., Haeuber, R., Tonnesen, G. S., Baron, J. S., Grossman-Clarke, S., Hope, D., and Sickman, J. O. 2003. Nitrogen emissions, deposition, and monitoring in the western United States. BioScience 53: 391-403.

Fenn, M.E., and Poth, M.A. 2004. Monitoring nitrogen deposition in throughfall using ion exchange resin columns: a field test in the San Bernadino Mountains. Journal of Environmental Quality 33: 2007–2014.

Fenn, M. E., Ross, C. S., Schilling, S. L., Baccus, W. D., Larrabee, M. A., and Lofgren, R. A. 2013. Atmospheric deposition of nitrogen and sulfur and preferential canopy consumption of nitrate in forests of the Pacific Northwest, USA. Forest Ecology and Management 302: 240-253.

Fenn, M. E., Sickman, J. O., Bytnerowicz, A., Clow, D. W., Molotch, N. P., Pleim, J. E., and

Campbell, D. H. 2009. Methods for measuring atmospheric nitrogen deposition inputs in arid and montane ecosystems of western North America. Developments in Environmental Science 9: 179-228.

Fowler, D., and M. H. Unsworth. 1984. Transfer to Terrestrial Surfaces [and Discussion]. Philosophical Transactions of the Royal Society of London. Biological Sciences 305B: 281–297.

Galloway, J. N. 1985. The Deposition of Sulfur and Nitrogen from the Remote Atmosphere Background Paper. In The biogeochemical cycling of sulfur and nitrogen in the remote atmosphere (pp. 143-175). Springer Netherlands.

Galloway, J. N., Townsend, A. R., Erisman, J. W., Bekunda, M., Cai, Z., Freney, J. R., ... & Sutton, M. A. (2008). Transformation of the nitrogen cycle: recent trends, questions, and potential solutions. Science 320: 889-892.

Geiser, L. H., Jovan, S. E., Glavich, D. A., & Porter, M. K. 2010. Lichen-based critical loads for atmospheric nitrogen deposition in Western Oregon and Washington Forests, USA. Environmental Pollution 158: 2412-2421.

George, E. F., Hall, M. A., and De Klerk, G. J. 2008. The components of plant tissue culture media I: macro-and micro-nutrients. In Plant propagation by tissue culture (pp. 65-113). Springer Netherlands.

Grantz, D. A., Garner, J. H. B., & Johnson, D. W. 2003. Ecological effects of particulate matter. Environment International 29: 213-239.

Halman, J. M., Schaberg, P. G., Hawley, G. J., & Eagar, C. 2008. Calcium addition at the

Hubbard Brook Experimental Forest increases sugar storage, antioxidant activity and cold tolerance in native red spruce (Picea rubens). Tree Physiology 28: 855-862.

Holland, E. A., Braswell, B. H., Sulzman, J., and Lamarque, J. F. 2005. Nitrogen deposition onto the United States and Western Europe: synthesis of observations and models. Ecological Applications 15: 38-57.

Hedin, L. O., J. J. Armesto, and A. H. Johnson. 1995. Patterns of Nutrient Loss from Unpolluted, Old-Growth Temperate Forests: Evaluation of Biogeochemical Theory. Ecology 76: 493–509.

Osada, R., Funkhouser, T., Chazelle, B., & Dobkin, D. 2002. Shape distributions. ACM Transactions on Graphics (TOG) 21: 807-832.

Herod, A. 2010. Scale. Routledge.

Hesp, P. A., Walker, I. J., Chapman, C., Davidson-Arnott, R., and Bauer, B. O. 2013. Aeolian dynamics over a coastal foredune. Prince Edward Island, Canada. Earth Surface Processes and Landforms.

Hicks, B. B., Hosker Jr, R. P., Meyers, T. P., & Womack, J. D. 1991. Dry deposition inferential measurement techniques—I. Design and tests of a prototype meteorological and chemical system for determining dry deposition. Atmospheric Environment. Part A. General Topics 25: 2345-2359.

Holland, D. M., Caragea, P., & Smith, R. L. 2004. Regional trends in rural sulfur concentrations. Atmospheric Environment 38: 1673-1684.

Holland, E. A., Braswell, B. H., Sulzman, J., and Lamarque, J. F. 2005. Nitrogen deposition onto

the United States and Western Europe: synthesis of observations and models. Ecological Applications 15: 38-57.

Jackson, P. S., & Hunt, J. C. R. 1975. Turbulent wind flow over a low hill. Quarterly Journal of the Royal Meteorological Society 101: 929-955.

Johnson, D. W., & Lindberg, S. E. 1992. Atmospheric deposition and forest nutrient cycling. A synthesis of the Integrated Forest Study. Springer-Verlag.

Kirchner, M., Fegg, W., Römmelt, H., Leuchner, M., Ries, L., Zimmermann, R., and Jakobi, G. 2014. Nitrogen deposition along differently exposed slopes in the Bavarian Alps. Science of the Total Environment 470: 895-906.

Körner, C. 2004. Mountain biodiversity, its causes and function. Ambio. 11.

Körner, C., Ohsawa, M., Spehn, E., Berge, E., Bugmann, H., Groombridge, B., ... & Yoshino, M. 2005. Mountain systems. Ecosystems and human well-being: current State and trends. Findings of the Conditions and Trends Working Group of the Millennium Ecosystem Assessment (R. Hassan, R. Scholes & N. Ash, eds.). Island Press, Washington DC, 681-716.

Katul, G. G., Cava, D., Siqueira, M., and Poggi, D. 2013. Scalar Turbulence within the Canopy Sublayer. Coherent Flow Structures at Earth's Surface 73-95.

Kelly, M., & Meentemeyer, R. K. 2002. Landscape dynamics of the spread of sudden oak death. Photogrammetric Engineering and Remote Sensing 68: 1001-1010.

Korhonen, L., Korpela, I., Heiskanen, J., & Maltamo, M. 2011. Airborne discrete-return LIDAR data in the estimation of vertical canopy cover, angular canopy closure and leaf area index. Remote Sensing of Environment 115: 1065-1080.

Latysh, N. E., and Wetherbee, G. A. 2012. Improved mapping of National Atmospheric Deposition Program wet-deposition in complex terrain using PRISM-gridded datasets. Environmental monitoring and assessment 184: 913-928.

Levia, D. F., and Frost, E. E. 2006. Variability of throughfall volume and solute inputs in wooded ecosystems. Progress in Physical Geography 30: 605-632.

Lim, K., Treitz, P., Wulder, M., St-Onge, B., & Flood, M. 2003. LiDAR remote sensing of forest structure. Progress in Physical Geography 27: 88-106.

Lindberg, S. E., Cape, J. N., Garten, C. T., & Ivens, W. 1992. Can sulfate fluxes in forest canopy throughfall be used to estimate atmospheric sulfur deposition? A summary of recent results. SE Schwartz and WGN Slinn, coordinators. Precipitation scavenging and atmosphere–surface exchange 3: 1367-1378.

Lindberg, S. E., & Garten, C. T. 1988. Sources of sulphur in forest canopy throughfall. Nature 336:148-151.

Lindberg, S.E., and G.M. Lovett. 1992. Deposition and Forest Canopy Interactions of Airborne Sulfur: Results from the Integrated Forest Study. Atmospheric Environment 26A: 1477–1492.

Lindberg, S. E., and Owens, J. G. 1992. Throughfall studies of deposition to forest edges and gaps in montane ecosystems. Biogeochemistry 19: 173-194.

Lovett, G. M., Arthur, M. A., Weathers, K. C., & Griffin, J. M. 2013. Effects of introduced insects and diseases on forest ecosystems in the Catskill Mountains of New York. Annals of the New York Academy of Sciences 1298: 66-77.

Lovett, G. M. 1994. Atmospheric Deposition of Nutrients and Pollutants in North America: An

Ecological Perspective. Ecological Applications 4: 629-650.

Lundquist, J. D., and Cayan, D. R. 2007. Surface temperature patterns in complex terrain: Daily variations and long-term change in the central Sierra Nevada, California. Journal of Geophysical Research 112:D11124.

Lyman, S. N., Gustin, M. S., Prestbo, E. M., Kilner, P. I., Edgerton, E., & Hartsell, B. 2009. Testing and application of surrogate surfaces for understanding potential gaseous oxidized mercury dry deposition. Environmental science & technology 43: 6235-6241.

Lyman, S. N., Gustin, M. S., Prestbo, E. M., & Marsik, F. J. 2007. Estimation of dry deposition of atmospheric mercury in Nevada by direct and indirect methods. Environmental Science & Technology 41: 1970-1976.

Makowski Giannoni, S., Rollenbeck, R., Fabian, P., and Bendix, J. 2013. Complex topography influences atmospheric nitrate deposition in a neotropical mountain rainforest. Atmospheric Environment 79: 385-394.

Matson, P., Lohse, K. A., & Hall, S. J. 2002. The globalization of nitrogen deposition: consequences for terrestrial ecosystems. AMBIO: A Journal of the Human Environment 31: 113-119.

Maurer, K. D., Hardiman, B. S., Vogel, C. S., and Bohrer, G. 2013. Canopy-structure effects on surface roughness parameters: Observations in a Great Lakes mixed-deciduous forest. Agricultural and Forest Meteorology 177: 24-34.

McClain, M. E., Boyer, E. W., Dent, C. L., Gergel, S. E., Grimm, N. B., Groffman, P. M., ... and Pinay, G. 2003. Biogeochemical hot spots and hot moments at the interface of terrestrial and aquatic ecosystems. Ecosystems 6: 301-312.

McDowell, W. H., C. G. Sánchez, C. E. Asbury, and C. R. R. Perez. 1990. Influence of Sea Salt Aerosols and Long Range Transport on Precipitation Chemistry at El Verde, Puerto Rico. Atmospheric Environment 24A: 2813–2821.

McNeill, J. R. 2003. The mountains of the Mediterranean world. Cambridge University Press.

McNeil, B. E., Read, J. M., & Driscoll, C. T. 2007. Foliar nitrogen responses to elevated atmospheric nitrogen deposition in nine temperate forest canopy species. Environmental science & technology 41:5191-5197.

McCune, B., Grenon, J., Mutch, L. S., & Martin, E. P. 2007. Lichens in relation to management issues in the Sierra Nevada national parks. Pacific Northwest Fungi 2: 1-39.

Meyers, T. P., Hicks, B. B., Hosker Jr, R. P., Womack, J. D., & Satterfield, L. C. 1991. Dry deposition inferential measurement techniques—II. Seasonal and annual deposition rates of sulfur and nitrate. Atmospheric Environment. Part A. General Topics 25: 2361-2370.

Menz, F. C., & Seip, H. M. 2004. Acid rain in Europe and the United States: an update. Environmental Science & Policy 7: 253-265.

Mikita, T., and Klimánek, M. 2010. Topographic exposure and its practical applications. Journalof Landscape Ecology 3: 42-51.

Nadkarni, N. M. 1986. The Nutritional Effects of Epiphytes on Host Trees with Special Reference to Alteration of Precipitation Chemistry. Selbyana 9: 44–51.

Nanus, L., Clow, D. W., Saros, J. E., Stephens, V. C., and Campbell, D. H. 2012. Mapping critical loads of nitrogen deposition for aquatic ecosystems in the Rocky Mountains, SA. Environmental Pollution 166: 125-135.

National Atmospheric Deposition Program (NADP). 2012. NRSP-3, Illinois State Water Survey, 2204 Griffith Dr., Champaign, Illinois 61820.

O'Brien, E. M., Field, R and Whittaker, R. J. 2000. Climatic gradients in woody plant (tree and shrub) diversity: water-energy dynamics, residual variation, and topography. Oikos 3: 588-600.

Noss, R. F. 1999. The redwood forest: history, ecology, and conservation of the coast redwoods. Island Press. Pajuste, K., Frey, J., & Asi, E. 2006. Interactions of atmospheric deposition with coniferous canopies in Estonia. Environmental Monitoring and Assessment 112: 177-196.

Pardo, L. H., Robin-Abbott, M. J., & Driscoll, C. T. 2011. Assessment of nitrogen deposition effects and empirical critical loads of nitrogen for ecoregions of the United States. Gen.

Pickering, C., Hill, W., and Green, K. 2008. Vascular plant diversity and climate change in the alpine zone of the Snowy Mountains, Australia. Biodiversity and Conservation 17: 1627-1644.

Plantegenest, M., Le May, C., & Fabre, F. 2007. Landscape epidemiology of plant diseases. Journal of the Royal Society Interface 4: 963-972.

Ponette-González, A. G., K. C. Weathers, and L. M. Curran. 2010. Tropical land-cover change alters biogeochemical inputs to ecosystems in a Mexican montane landscape. Ecological Applications 20: 1820–1837.

Porter, E., Blett, T., Potter, D. U., and Huber, C. 2005. Protecting resources on federal lands: Implications of critical loads for atmospheric deposition of nitrogen and sulfur. BioScience 55: 603-612.

Pugnaire, F. I., and Luque, M. T. 2001. Changes in plant interactions along a gradient of environmental stress. Oikos 93: 42-49.

Rizzo, D. M., & Garbelotto, M. 2003. Sudden oak death: endangering California and Oregon forest ecosystems. Frontiers in Ecology and the Environment 1: 197-204.

Schaberg, P. G., DeHayes, D. H., Hawley, G. J., Murakami, P. F., Strimbeck, G. R., & McNulty, S. G. 2002. Effects of chronic N fertilization on foliar membranes, cold tolerance, and carbon storage in montane red spruce. Canadian Journal of Forest Research 32: 1351-1359.

Schlesinger, W. H., & Bernhardt, E. S. 2013. Biogeochemistry: an analysis of global change. Academic press.

Schmitt, M., Thöni, L., Waldner, P., & Thimonier, A. 2005. Total deposition of nitrogen on Swiss long-term forest ecosystem research (LWF) plots: comparison of the throughfall and the inferential method. Atmospheric Environment 39: 1079-1091.

Seinfeld, J. H., and Pandis, S. N. 2012. Atmospheric chemistry and physics: from air pollution to climate change. John Wiley & Sons.

Skole, D. L. 2004. Geography as a great intellectual melting pot and the preeminent interdisciplinary environmental discipline. Annals of the Association of American Geographers 94: 739-743.

Stankwitz, C., Kaste, J. M.,and Friedland, A. J. 2012. Threshold increases in soil lead and mercury from tropospheric deposition across an elevational gradient. Environmental science & technology. 46: 8061-8068.

Su, H. B., Schmid, H. P., Vogel, C. S., & Curtis, P. S. 2008. Effects of canopy morphology and

thermal stability on mean flow and turbulence statistics observed inside a mixed hardwood forest. agricultural and forest meteorology 148: 862-882.

Sayre, N. F. 2005. Ecological and geographical scale: parallels and potential for integration. Progress in Human Geography *29*:276-290.

Takemoto, B. K., Bytnerowicz, A., & Fenn, M. E. 2001. Current and future effects of ozone and atmospheric nitrogen deposition on California's mixed conifer forests. Forest Ecology and Management 144: 159-173.

Turner, W., Spector, S., Gardiner, N., Fladeland, M., Sterling, E., & Steininger, M. (2003). Remote sensing for biodiversity science and conservation. Trends in ecology & evolution 18: 306-314.

Vitousek, P. 1982. Nutrient cycling and nutrient use efficiency. American Naturalist. 553-572.

Vitousek, P. M. 1984. Litterfall, nutrient cycling, and nutrient limitation in tropical forests. Ecology 65: 285-298.

Weathers, K. C., and A. G. Ponette- González. 2011. Atmospheric deposition. Pages 357-370 in D. Levia, D. Carlyle-Moses, and T. Tanaka, editors. Forest Hydrology and Biogeochemistry: Synthesis of Past Research and Future Directions. Springer, New York, New York, USA

Weathers, K. C., Lovett, G. M., & Likens, G. E. 1995. Cloud deposition to a spruce forest edge. Atmospheric Environment 29: 665-672.

Weathers, K. C., and G. M. Lovett. 1998. Acid Deposition Research and Ecosystem Science:

Synergistic Success. Pages 195-219 in M.L. Pace and P.M. Groffman, editors. Success, Limitations, and Frontiers in Ecosystem Science, Springer-Verlag, New York, New York, USA

Weathers, K. C., G. M. Lovett, G. E. Likens, and R. Lathrop. 2000. The Effect of Landscape Features of Deposition to Hunter Mountain Catskill Mountains. New York. Ecological Applications 10: 528-520.

Weathers, K.C., and G. E. Likens. 2006a. Acid Rain. Pages 1507-1520 in W.N. Rom, editor. Environmental and occupational medicine. Fourth edition. Lippincott Williams and Wilkins, Philadelphia, Pennsylvania, USA.

Weathers, K. C., S. M. Simkin, G. M. Lovett, and S. E. Lindberg. 2006b. Empirical Modeling of Atmospheric Deposition in Mountainous Landscapes. Ecological Applications 16: 1590-1607.

Weathers, K.C., M. L. Cadenasso, and S.T. A. Pickett. 2001. Forest Edges as Nutrient and Pollutant Concentrators: Potential Synergisms Between Fragmentation, Forest Canopies, and the Atmosphere. Conservation Biology 15: 1506-1514.

Zhang, L., Jacob, D. J., Knipping, E. M., Kumar, N., Munger, J. W., Carouge, C. C., ... and Chen, D. 2012. Nitrogen deposition to the United States: distribution, sources, and processes. Atmospheric Chemistry and Physics Discussions 12:241-282.

Zimmermann, F., Lux, H., Maenhaut, W., Matschullat, J., Plessow, K., Reuter, F., and Wienhaus, O. 2003. A review of air pollution and atmospheric deposition dynamics in southern Saxony, Germany, Central Europe. Atmospheric Environment 37: 671-691.